THE ASTROPHYSICAL JOURNAL

AN INTERNATIONAL REVIEW OF SPECTROSCOPY AND ASTRONOMICAL PHYSICS

VOLUME 89 MAY 1939 NUMBER 4

A METHOD FOR THE DETERMINATION OF STELLAR DIAMETERS[1]

J. D. WILLIAMS

ABSTRACT

It has been suggested at various times that the angular diameter of a star may be deduced from a study of its light-curve while it is undergoing occultation by the moon; but Eddington has shown that observation of the geometrical occultation is almost hopelessly complicated by diffraction effects, except for stars of very large angular diameter. The present paper points out that the diameter may be deduced from the diffraction effect itself, and the question is discussed quantitatively.

MacMahon has proposed[2] that the diameters of stars be investigated by determining the time interval required for their occultation by the moon. Eddington drew attention[3] to the diffraction effect and estimated that this would cause a point star to have a spurious diameter of 0".008; consequently, the approach to the problem from the viewpoint of geometrical optics is rather hopeless except in the case of a star with a very large angular diameter. The observation in the latter case has been attempted[4] recently at Cambridge and at Paris, the star being Antares.

It has occurred to the writer that the diffraction effect, which seems destined to close the direct line of investigation, may be used to forward the inquiry; at least this possibility emerges when the

[1] Presented at the sixtieth meeting of the American Astronomical Society, at Ann Arbor, Michigan.

[2] *M.N.*, **69**, 126, 1908–1909.

[3] *M.N.*, **69**, 178, 1908–1909.

[4] *Nautical Almanac, 1939*, Suppl., p. 1, n.

problem is idealized in the following manner: if we assume that the effect of the moon, so far as diffraction is concerned, is the same as that of a plane screen perpendicular to the line of sight and situated so that its edge is tangent to the moon's limb at the point where occultation occurs, the phenomenon is reduced to the familiar problem of diffraction at a straight edge. For a point source of light, the intensity of illumination increases from zero within the geometrical shadow of the screen, attains one-fourth the intensity of the free wave at the edge, and beyond the shadow exhibits a series of oscillations which converge rapidly to the intensity of the free wave. The point to be raised is simply that the character of the oscillations for light from an extended source is not the same as for a point source and that it depends, in a predictable manner, on the diameter of the source. Actually the problem may be inverted so that if the variation of intensity in the fringes is observed, we may estimate the diameter of the star.

For a point source the intensity J is given by[5]

$$8J = (1 \pm 2F_1)^2 + (1 \pm 2F_2)^2 , \qquad (1)$$

the upper signs corresponding to points outside the shadow, the lower to points within it; the unit of intensity is that of the free wave. The functions F_1 and F_2 are Fresnel's integrals,

$$\int_0^v \cos \frac{\pi}{2} v^2 dv \qquad \text{and} \qquad \int_0^v \sin \frac{\pi}{2} v^2 dv ,$$

which have been computed and tabulated. For the case under discussion the scale of the phenomenon is remarkable, as may be seen from the following list of the abscissas x (in meters), measured from the geometric edge of the shadow, corresponding to the first few maxima and minima:

Maxima	11.0	21.2	27.8
Minima	16.9	24.7	....

[5] Cf. Preston, *Theory of Light* (4th ed.), p. 296.

The values for the moon's distance D and the wave length of light λ used in obtaining them were 3.8×10^8 and 4.3×10^{-7} meters, the formula[6] being

$$x = v\sqrt{\frac{D\lambda}{2}}.$$

The values of v at the turning-points are given by Fresnel.

The positions of the fringes predicted by theory have been verified by observation many times, but the relative intensities have not been substantiated quantitatively until Lyman's recent work.[7]

The writer has sought to obtain by approximate methods the intensity-curves corresponding to circular light sources of finite but angularly small diameters. A table of the values of J in equation (1) was prepared for values of the argument v differing by $\Delta v = 0.1$. The desired effect at the point $v = v_0$ was then found from

$$I(v_0, n) = C\int J(v) f(v, v_0, n)dv\,, \qquad (2)$$

where

$$f^2 = n^2\Delta v^2 - (v - v_0)^2\,,$$

the limits of integration being $v_0 + n\Delta v$ and $v_0 - n\Delta v$; C determines the unity of intensity. The integration was performed numerically by Simpson's method for several small values of n. $\Delta v = 0.1$ corresponds to $0''.0005$ displacement of a point source, so integration over the range $2n\Delta v$ represents a circular source of diameter $n/1000$ seconds of arc. In Figure 1 the curves are shown for a point source and for one of diameter $0''.004$, the range in v being from 0 to 3. Curves for other values of n have been omitted so as to simplify the diagram.

It will be observed that the two light-curves differ considerably, which does not seem, at first sight, to be consistent with Lyman's[8]

[6] Fresnel, *Œuvres completes*, p. 323, 1866.

[7] *Proc. Nat. Acad. Sci.*, **16**, 71, 1930.

[8] *Op. cit.*

verification of classical theory. But while Lyman's light source was 1".37 when he confirmed the point-source theory, the other constants of his apparatus were such as to cause integration over a range in v of 0.0175 only.

If observations of this effect can be secured, the method promises to rival the stellar interferometer in power. This last sentence brings us squarely to the crux of the matter, namely, the technical difficulties. The observations would consist of measuring and re-

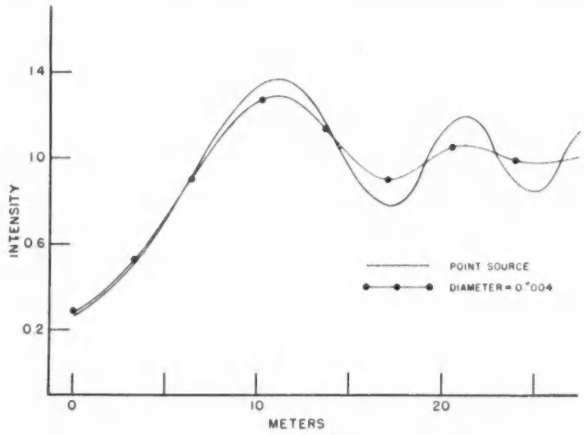

FIG. 1

cording the light intensity as the moment of occultation approaches. Since the telescope will pass along the fringes at a rate of 1 meter in about 0s.0015, the instruments must be capable of high-speed performance as well as high sensitivity. However, these criteria are well within the limits of time lag and change of reaction to change of stimulus associated with photoelectricity, so that the observation is conceivable. Perhaps conjunction of the photoelectric cell and the cathode-ray oscillograph would make it a reality.

The present discussion of the subject is intentionally brief and crude, since it does not seem worth while to examine it elaborately unless observations of this type are actually attempted. In any event, theory would be much restricted by the complexity of conditions on the limb of the moon, although it may be indicated that we need be concerned only with a small surface on the moon, since a

cone of light with vertex angle 0".0006 is only 1 meter across at that distance. But there remain such disturbing possibilities as a reflection effect.

Finally, the observation probably should not be attempted with a telescope of aperture much less than 1 meter, so that atmospheric effects will be integrated out, a suggestion due to R. O. Redman[9] and based upon consideration of the separation of shadow bands.

I am indebted to Professor H. N. Russell, who mentioned that the geometrical problem was beset with diffraction difficulties.

PRINCETON UNIVERSITY OBSERVATORY
August 15, 1938

[9] Personal communication.

PHOTOELECTRIC OBSERVATION OF DIFFRACTION AT THE MOON'S LIMB*

A. E. WHITFORD

ABSTRACT

The occultations of β Capricorni and ν Aquarii on September 6 and 7 (respectively), 1938, were observed with the 100-inch telescope and a fast photoelectric system. The record was obtained by photographing the screen of a cathode-ray tube with a moving-film camera. An analysis of the unavoidable noise present in amplifiers predicted fluctuations of approximately the magnitude observed, about 4 per cent of the brightness of β Capricorni.

A calculation of the diffraction effects to be expected was carried out, with allowance for the wide range of wave lengths used. The observations were in satisfactory agreement with the calculation. The stars were not large enough to change the diffraction pattern from that due to a point source by an observable amount. Therefore, no information on stellar diameters was obtained. With stars of angular diameters greater than $0''.005$, the method can be used to measure stellar diameters.

The possibility of determining the diameter of a star by measuring the time for it to pass behind the dark limb of the moon has occurred independently to several astronomers in the last thirty years, of whom MacMahon[1] seems to have been the first. The problem immediately resolves itself into two parts: first, the technical question of whether it is feasible to obtain observations of the variation in intensity of the light of a star occurring in a time interval of about 0.01 sec; and second, the consideration of the influence of diffraction on the intensity changes to be expected. The technical question will be taken up first.

The most favorable occultations during 1938 were those of β Capricorni ($3^{m}.25$, composite spectrum Go + Ao) and ν Aquarii ($4^{m}.52$ Ko) on September 6 and 7, respectively. The plan of observation was to let the light fall on a photoelectric cell at the focus of the 100-inch reflector, amplify the variations in a four-stage alternating-current amplifier with a voltage gain of about 10^{5}, and apply the output to the vertical deflecting plates of a 3-inch cathode-ray oscilloscope. The oscillations of the luminous spot were photographed

* *Contributions from the Mount Wilson Observatory, Carnegie Institution of Washington*, No. 610.

[1] *M.N.*, **69**, 126, 1909.

with a moving-film camera,[2] using an f: 1.5 lens of 25 mm focus. The cathode-ray spot moved only in a vertical direction; the time coordinate was supplied by the motion of the film. The film speed was 450 mm/sec. By using a spiral motion of the drum similar to that on seismographs, about 75 feet of trace could be recorded on a 3-foot piece of 35-mm film. There was a tenfold reduction between cathode-ray screen and film.

This general scheme has been used to record phenomena much faster than those here encountered, but always with a considerably greater amount of light than that available from a star even with a large telescope. As the intensity of the light is reduced, more amplification is necessary, and finally the signal is no larger than the unavoidable background noise present in all amplifiers.

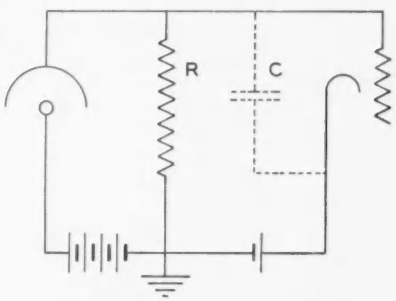

FIG. 1.—Input circuit of amplifier

Figure 1 shows schematically the input circuit of the amplifier. The condenser C, indicated by the dotted lines, represents the sum of the capacities of the photocell and connections and the dynamic input capacity of the first tube. If K is the sensitivity constant of the photocell in amperes per lumen, the signal voltage appearing across the input resistor R when a luminous flux L is stopped or started is

$$E_s = KLR\,. \tag{1}$$

It is assumed that the signal can be represented with the required accuracy, as the sum of sinusoidal waves of frequencies less than $f_0 = 1/2\pi RC$.

On the assumption that noise produced by external disturbances, such as stray electric or magnetic fields, vibration, poor connections, and the like, has been eliminated, there will remain inherent and unavoidable fluctuations arising principally from thermal agitation of electricity in the resistor R. In this case, shot effects of grid and

[2] Through the courtesy of Dr. J. A. Anderson this camera was constructed in the machine shop of the 200-inch telescope of the California Institute of Technology.

photo currents in the input circuit and "tube noise" can be made negligible in comparison with thermal noise by proper choice of the first tube and its operating potentials. As shown by Nyquist,[3] the thermal noise voltage is given by

$$\overline{E_n^2} = 4kT \int_0^\infty R(f)df\,, \tag{2}$$

where f is the frequency, $R(f)$ the resistive component of the input impedance as a function of frequency, T the absolute temperature, and k the Boltzmann constant. For our case, $R(f) = R/(1 + 4\pi^2R^2C^2f^2)$. In the amplifier here used, the interstage coupling condensers were rather large, so that the low-frequency cutoff was at about 1 cycle per second. The high-frequency response was kept flat to a frequency several times higher than the critical frequency $f_0 = 1/2\pi RC$ determined by the capacity shunt in the input circuit. Therefore, the amplifier does not appreciably limit the spectrum of noise frequencies, and the noise in the input circuit will be faithfully reproduced in the output circuit, where the observation is made. Hence, it is permissible merely to insert the value of $R(f)$ in equation (2) and carry out the integration. The result is[4]

$$\overline{E_n^2} = \frac{kT}{C}\,. \tag{3}$$

A numerical calculation can now be made. The total capacity in the input circuit was estimated to be 10 micromicrofarads, or 10^{-11} farads. At 300° K the noise voltage then comes out to be 2×10^{-5} *RMS* volts. The signal voltage for a given light-intensity increases directly with R, but the critical frequency f_0 at which the response drops off seriously, varies inversely as R. Whether a satisfactory compromise is possible depends on the amount of light available. The resistance actually used had a value of 2×10^7

[3] *Phys. Rev.*, **32**, 110, 1928. See also J. B. Johnson, *ibid.*, 97; G. L. Pearson, *Physics*, **5**, 233, 1934; E. A. and A. G. Johnson, *Phys. Rev.*, **50**, 171, 1936.

[4] This result was first derived by Hafstad (*Phys. Rev.*, **44**, 201, 1935) for a direct-current amplifier using an electrometer tube; but, so far as the writer is aware, it has not been pointed out that it applies to wide-band alternating-current amplifiers where the high-frequency response is limited only by the input circuit.

ohms, making the critical frequency f_0 about 800 cycles. A candle at a distance of 1 km is equivalent[5] to a star of visual magnitude +0.8. Then it may be calculated that β Capricorni, visual magnitude 3.25, would, after allowing for losses in the atmosphere and three reflections from aluminum mirrors, furnish 3×10^{-7} lumens at the focus of the 100-inch telescope. For radiation from a black body at 6000° K, the sensitivity constant of a gas-filled cesium oxide photocell is about 75×10^{-6} amperes per lumen. Then the signal voltage $E_s = 4.5 \times 10^{-4}$ volts. The signal-to-noise ratio would then be

$$\frac{E_s}{(\overline{E_n^2})^{1/2}} = \frac{4.5 \times 10^{-4}}{2 \times 10^{-5}} = 22.5 ,$$

which is a reasonably satisfactory value. For ν Aquarii, which gives a third as much light, the ratio would be only fair.

The RCA 921 phototube was selected because of its non-microphonic construction, its low capacity, and its superior high-frequency response, compared with other gas-filled cells. The first two tubes of the amplifier were RCA 1603's, operated with the screen at 22.5 volts and the plate at about 45 volts, the plate supply being from the same 90-volt battery as that used for the phototube. The 1603's were chosen primarily because of their low microphonic sensitivity, but they had a satisfactorily small grid current as well. It was necessary to include a triode stage in the part of the amplifier at the end of the telescope in order to get the signal into a relatively low-impedance circuit before sending it through the 40-foot cable leading from the Cassegrain focus to the oscilloscope and its self-contained vertical amplifier. Otherwise the capacity of the cable would have shunted out the higher frequencies. A 6L5-G tube was used.

The observations were made successfully on the two nights as planned. One observer at the Cassegrain focus of the telescope checked the following of the telescope for some minutes and made sure that the star image was central in the focal-plane diaphragm up to about 40 seconds before immersion, when the guiding prism was pulled out and the light admitted to the photocell. The diaphragm had a radius of about 1.2 mm, or 6″; the angular distance to the

[5] Russell, Dugan, and Stewart, *Astronomy*, p. 612, Ginn & Co., 1927.

terminator was about 45″ on each night. Other diaphragms were inserted along the beam to reduce the amount of scattered moonlight. A second observer watched the occultations in the finder, and a third operated the oscilloscope and camera. The writer is indebted to Dr. James Robertson, director of the Nautical Almanac Office, for

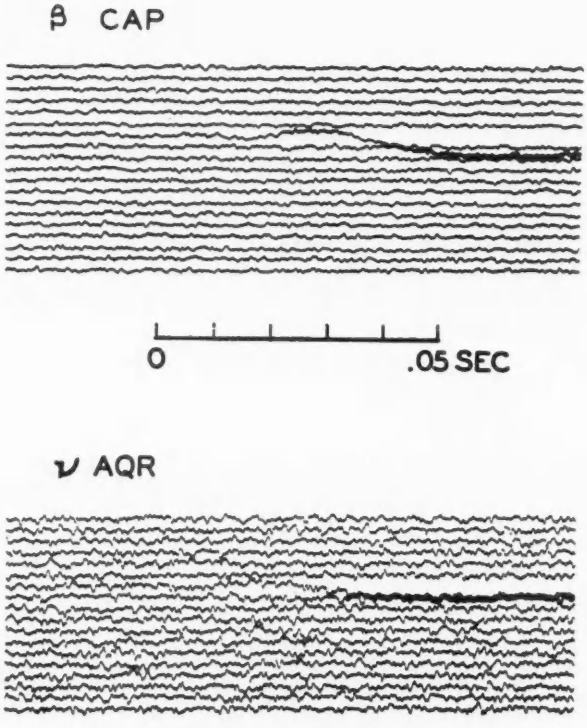

FIG. 2.—Observed variation in the light of β Capricorni and ν Aquarii as they disappeared behind the dark limb of the moon. These are 2-inch sections of a spiral trace 36 inches in circumference. Time increases from right to left and from the bottom to the top.

furnishing calculations of the times of the occultations from more accurate data than those given in the *Ephemeris*. The predictions were accurate to about 2 seconds. The camera was started 20 seconds before the predicted time, to provide a wide margin of safety.

The observed curves of light-variation are shown in Figure 2. These represent 2-inch sections of the entire 36-inch film. The lower

traces in each film represent the time before occultation; the upper traces, the time after occultation. Any difference in stability should represent the influence of seeing. It is seen that the difference is small. This result may be ascribed to the averaging effect of the 100-inch mirror on the atmospheric waves.

Although spread out too much in the time co-ordinate, the traces immediately suggest diffraction at a straight edge. This possibility had not been sufficiently considered by the writer prior to the time of observation, although it had been mentioned by Eddington[6] in 1909 immediately following MacMahon's proposal. Very recently J. D. Williams[7] has published an analysis of the diffraction problem and suggested that the small changes in the pattern caused by the finite diameter of the source could be used as a gauge of the angular diameter of stars. The writer's computation of the expected diffraction effects was well along before he learned of Williams' work. The conclusions are the same, and hence the details will not be repeated.

Williams considers only the case of monochromatic light, and for comparison with experiment an extension to the case of a source emitting a continuous spectrum is necessary. Figure 3 shows the effective spectral response-curve of the photocell obtained by multiplying together the spectral response-curve of the *Cs-O-Ag* cathode for an equal-energy source, the energy-curve for a black body at 6000° K, and the absorption in the earth's atmosphere. The altitude of β Capricorni at the time of occultation was 20°, corresponding to an air mass 2.92 times the vertical mass. Only the Go component of β Capricorni is bright enough over most of the wave-length range to be effective; the Ao component is therefore neglected. The analysis will be carried out in detail only for β Capricorni on account of the poor signal-to-noise ratio for ν Aquarii. The results are qualitatively the same for the two stars.

To reduce the labor of computing the diffraction pattern for many wave lengths, the spectral response-curve was divided into five parts of approximately equal width. The area and centroid of each part was found. The heavy vertical lines in Figure 3 represent the five

[6] *M.N.*, **69**, 178, 1909.

[7] *Ap. J.*, **89**, 467, 1939. The writer is indebted to Mr. Williams for the opportunity of examining his results prior to publication.

monochromatic sources that were computed to represent the whole curve. This rather coarse lumping is not as bad as it looks, since the parameter which determines the scale of the diffraction pattern is proportional to the square root of the wave length.

Five diffraction-curves were computed by reading off points on a standard curve plotted by the Cornu-spiral method.[8] The five curves

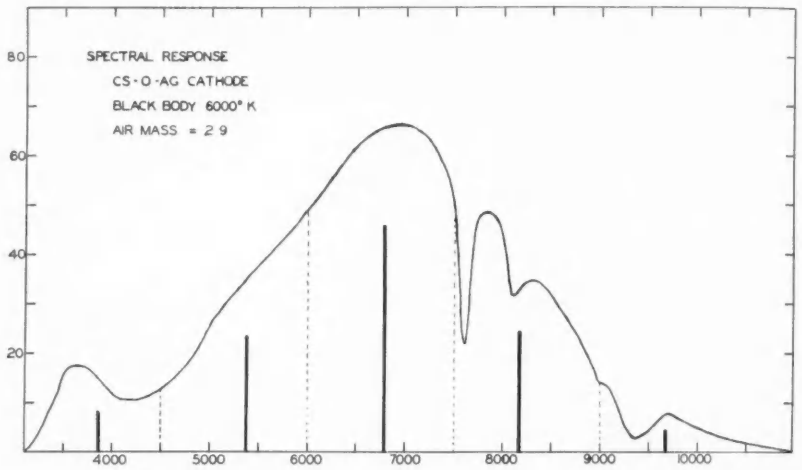

FIG. 3.—Effective spectral response-curve of a cesium-oxide photocell, allowing for the energy-curve of the star and the absorption in the earth's atmosphere. The curve is lumped into five monochromatic sources, indicated by the heavy vertical lines.

were then added, and the integrated result is shown in Figure 4. This, of course, applies to a point source. To take account of the finite diameter of the star, it is sufficient as a first approximation to resolve it into an equivalent double with a separation equal to the distance between the centers of intensity of the two halves of the star.[9] For a uniform disk this is 41 per cent of the diameter; darkening at the limb equal to that of the sun reduces it to 35 per cent. For β Capricorni the calculated equivalent double star has a separation of the order of $0''.001$, which, viewed from the moon's limb, is a distance of 180 cm on the earth. The intensity would then be repre-

[8] See, e.g., Jenkins and White, *Fundamentals of Physical Optics*, p. 193, McGraw-Hill, 1937.

[9] Russell, Dugan, and Stewart, *op. cit.*, p. 745.

sented by the sum of two identical point-source curves, one for each component of the hypothetical double, but with one curve displaced laterally 180 cm with respect to the other. The resultant is indicated by the dotted lines. It has been moved horizontally into the best fit with the original curve, because, since the time is not known absolutely, only the change in the shape of the curve will be observable.

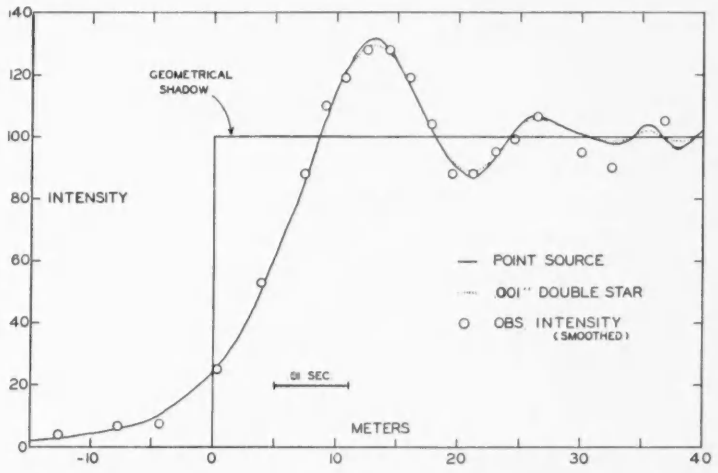

FIG. 4.—Comparison of computed and observed diffraction pattern. The telescope scans the curve from right to left.

It is seen that the distortion is not large enough to be observable with certainty; if the star had been twice as large, it would have produced an effect above the threshold of observation. When the separation of the two hypothetical components is small, the departure from the original curve at the most sensitive points, the points of maximum curvature, is proportional to the square of the separation.

The computed noise level indicated an *RMS* error of about 4 per cent of the whole intensity of the star for a single instantaneous observation, which checked roughly with the observed values. The observed points in the figure have a smaller error than this because they were taken from a smooth curve drawn through the original record in the same way that a smooth curve is drawn through the plate-grain irregularities on a microphotometer trace. The points

were fitted by sliding and stretching in a horizontal direction only. The observed speed of the fringes past the telescope was 613 meters/sec, as compared with a computed speed of 541 meters/sec. The calculated angle between the moon's limb and the path of the star was 42°.9. The observed speed would correspond to an angle of 50°.5, or a slope of 7°.6 on the lunar surface. Such a slope seems not unreasonable. The occultation took place at a relatively smooth part of the moon's limb. In the mountainous regions a steeper slope might have been encountered. Although it might be anticipated that the assumption that the moon's limb is a straight edge would turn out to be too optimistic, the observations on the two stars did not show any contradiction of this hypothesis.

The diffraction-curve is not scanned by an infinitely narrow slit, and some distortion might arise from the use of a large telescope. At any particular instant the 100-inch telescope would receive light from a portion of the diffraction-curve 250 cm wide. In order to estimate the averaging effect, it is sufficient to replace the telescope by an "equivalent double," as was done for the star disk. The result is a separation of about 105 cm on the earth, as compared with 180 cm for β Capricorni; the effect is therefore negligible. With the 200-inch telescope, however, the distortion might be troublesome.

If a potassium hydride photocell as free from microphonic sensitivity and with as low time-lag as the type of gas-filled cesium oxide cell (RCA 921) actually used can be obtained, it would operate with a much narrower range of wave lengths. The peaks of the diffraction-curve would then be sharper and more sensitive to distortion by sources of small equivalent separation. Against this must be set the poorer response of potassium-hydride cells to red stars, which are, of course, the only favorable cases. Some improvement in signal-to-noise ratio could be realized by using a larger value of the input resistor. An inspection of Figure 4 shows that the highest frequency in the observed diffraction pattern was not over 100 cycles per second. To record this with negligible phase distortion in the amplifier, it would be necessary to have the critical frequency f_0 be of the order of 300 cycles, but not as high as 800 cycles, which was the value in the amplifier actually used. A gain of a factor of 2 or 3 is possible here. Beyond that the prospect for improvement in ob-

servational accuracy seems not very hopeful. It may be remarked that the calculation of the signal-to-noise ratio rests on such general considerations that it applies to electrometers or to any device where the current is sent through a resistance to obtain a voltage. There is theoretically a possibility of some improvement by the use of secondary emission multipliers, but a trial of two types failed to reveal anything as good as the conventional methods of amplification for this particular problem.

The moon, in all positions of its orbit, occults about a dozen stars whose angular diameters, calculated from their magnitudes and spectra, are larger[10] than $0''.005$. For these stars there appears to be a definite hope of obtaining an experimental measure of the diameter by observing the diffraction pattern at the time of occultation.

The writer is indebted to Dr. Joel Stebbins for an accurate calculation of the speed of the shadow past the telescope, as well as for helpful advice and encouragement; to Mr. A. H. Joy for giving time on the 100-inch telescope; and to Messrs. D. O. Hendrix and Glenn Moore for assistance with the manipulations in the dome. This work was supported in part by the Wisconsin Alumni Research Foundation and the Observatory Council of the California Institute of Technology.

CARNEGIE INSTITUTION OF WASHINGTON
MOUNT WILSON OBSERVATORY,
WASHBURN OBSERVATORY
UNIVERSITY OF WISCONSIN
February 1939

[10] For a giant star to have an angular diameter greater than $0''.005$ it must be brighter than $1^m.65$ for spectral class Go, brighter than $3^m.50$ for class Ko, and brighter than $6^m.0$ for class Mo. These are visual magnitudes and are calculated from the equation in Russell, Dugan, and Stewart, *op. cit.*, p. 612.

SECOND REPORT ON THE EXPANSION OF THE CRAB NEBULA*

JOHN C. DUNCAN

ABSTRACT

The expansion of the Crab nebula, revealed in 1921 by a comparison of the positions of twelve nebulous points on photographs made with the 60-inch telescope with an interval of 11.5 years, is now studied by observing twenty points on photographs made with the 60-inch with an interval of 29.1 years. On the assumption that the observed nebulous points started simultaneously and that each has moved with uniform velocity, the point from which the expansion takes place is located 20″ following and 2″ south of the northern component of the central double star, and the date of the outburst is indicated as A.D. 1172. The observed angular motions, together with the radial velocities published by Mayall, indicate for the nebula a distance of about 4200 light-years and a major axis of about 6. There is evidence that the nebula has a proper motion of 0″.037 per year, corresponding to a velocity across the line of sight of 230 km/sec.

The south component of the central double star has a proper motion of 0″.019 per year, while the north component is sensibly stationary. A twelfth-magnitude star situated 5′.8 north-preceding the nebula has the conspicuous proper motion of 0″.240 per year.

Outward motions of twelve luminous condensations situated near the periphery of the Crab nebula (NGC 1952 = M 1 Tauri) were reported in 1921.[1] These motions were determined by comparing with each other two plates made at the Newtonian focus of the 60-inch reflector, one by Ritchey in 1909 and the other by me 11.5 years later. Recently I have made similar photographs of this unique object, which, together with the earlier plates, show the expansion more clearly. The best of these was made on November 24, 1938, with an exposure of 1 hour on an Imperial Eclipse plate; and the results now reported were obtained from a comparison of this plate with Ritchey's, the interval being 29.1 years. The measurements were made on the blink comparator constructed at this observatory, which is superior to the instrument formerly used; and this circumstance, the longer interval, and the superiority of the photograph of 1938 over that of 1921 combine to make the present results much the more trustworthy.

The co-ordinates x and y refer to rectangular axes intersecting at

* *Contributions from the Mount Wilson Observatory, Carnegie Institution of Washington*, No. 609.

[1] J. C. Duncan, *Mt. W. Comm.*, No. 76; *Proc. Nat. Acad. Sci.*, **7**, 179, 1921.

PLATE XXIV

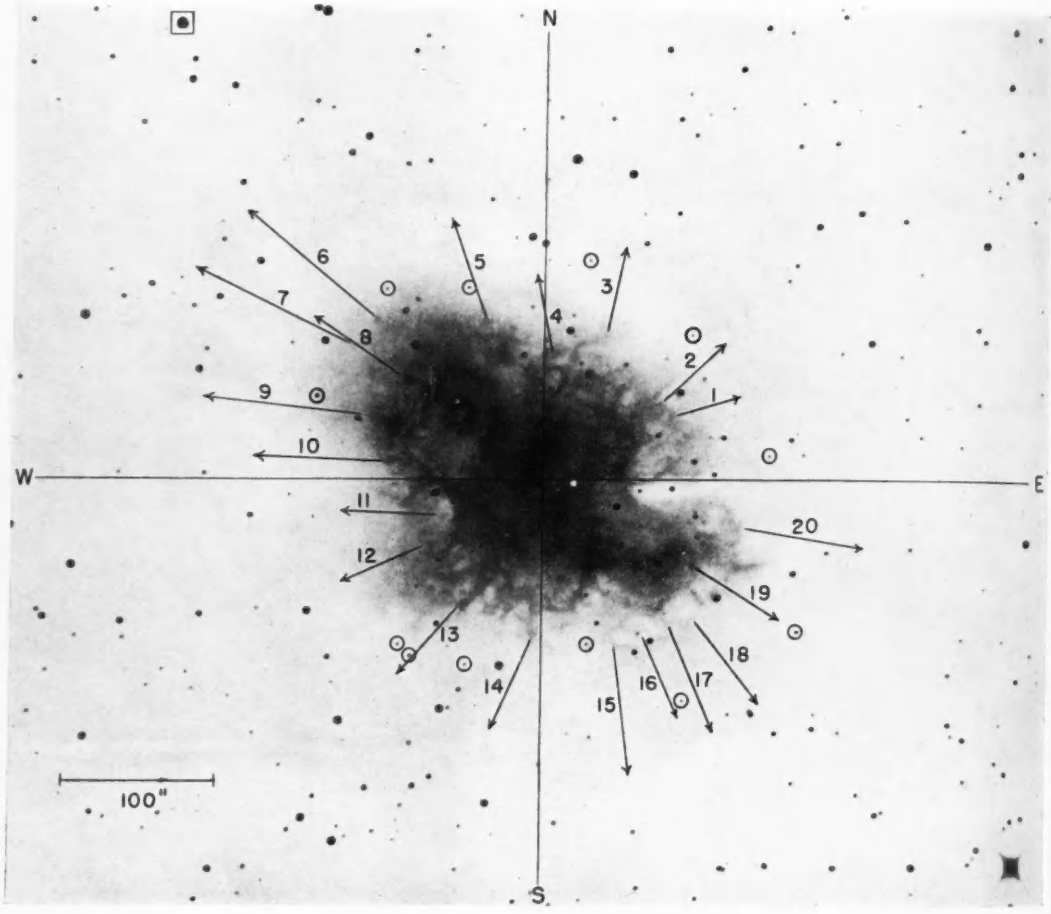

EXPANSION OF THE CRAB NEBULA

The vectors indicate the motion of twenty nebulous points in 500 years. Projected backward they suggest an outburst occurring about 800 years ago at the point marked by the white spot. Comparison stars are encircled.

the north component of the sixteenth-magnitude double star near the center of the nebula and approximately coinciding with a parallel of declination and an hour circle. The plate constants were determined from measurements on twelve stars of the seventeenth and eighteenth magnitude, not chosen, as before, near the measured nebulous points but situated three in each quadrant and far enough from the origin to be free from nebulosity. The probable error of a measurement of a comparison star, including any relative proper motion, is $\pm 0''.070$ in x and $\pm 0''.066$ in y. The components of the

TABLE 1

ANNUAL MOTIONS WITHIN THE CRAB NEBULA

Point	x	Δx	y	Δy	Point	x	Δx	y	Δy
1.....	+ 88″	+0″.094	+ 40″	+0″.029	11....	− 70″	−0″.130	− 24″	+0″.004
2.....	+ 82	+ .084	49	.078	12....	− 77	− .109	44	− .051
3.....	+ 42	+ .026	93	.110	13....	− 53	− .076	82	− .089
4.....	+ 3	− .023	83	.105	14....	− 5	− .053	103	− .091
5.....	− 40	− .042	108	.130	15....	+ 51	+ .024	110	− .168
6.....	−113	− .171	108	.141	16....	+ 63	+ .054	101	− .107
7.....	−128	− .208	89	.103	17....	+ 85	+ .057	98	− .141
8.....	− 91	− .120	65	.084	18....	+102	+ .089	96	− .112
9.....	−116	− .216	41	.029	19....	+102	+ .120	58	− .068
10.....	−104	−0.172	+ 10	+0.006	20....	+134	+0.162	− 30	−0.024

central double star were also measured. The north component betrayed no proper motion as great as the probable error, but the south component moves in the direction of diminishing right ascension at a rate of $0''.019$ per year. A twelfth-magnitude star, No. 177 on Chart 402 of the Paris *Carte du ciel*, situated $4'.0$ preceding and $4'.7$ north of the origin of co-ordinates in 1938 (inclosed in a square on Pl. XXIV) has a proper motion $\Delta x = -0''.058$, $\Delta y = -0''.229$, per year. No other conspicuous stellar proper motions were found on the plates.

Twenty nebulous points were measured, with the results shown in Table 1, where the displacements are given in seconds of arc per year, and in Plate XXIV, where the vectors represent the motions which, at the observed rate, would take place in 500 years. On Plate XXIV the comparison stars are encircled.

On the assumptions that all particles of the expanding nebula started from the same small region at the same time and that each

has since moved with uniform velocity (though not all with the same velocity) relative to the background of stars, the apparent motion of each measured nebulous point should conform to an equation of the type

$$x - x_0 = t\Delta x ,$$

where x is its co-ordinate in 1938 in seconds of arc, x_0 the corresponding co-ordinate of the point of outburst, t the time in years since the explosion, and Δx the displacement in seconds per year revealed by the measurements. From solutions of the twenty equations in x and the twenty in y there result the following values:

$$x_0 = +20''.3 \pm 2''.2 , \qquad t = 740 \pm 19 \text{ years} ,$$
$$y_0 = -\ 1''.8 \pm 2''.0 , \qquad t = 793 \pm 23 \text{ years} .$$

The point of explosion thus determined is indicated on Plate XXIV by a white dot having a radius approximately equal to its probable error. The present center of the nebula is obviously on the opposite side of the origin.

The region of the present center is the bright portion in which Lampland made the original discovery[2] that the nebula was changing; but ordinary blue-sensitive plates reveal here no measurably definite details and so, while they plainly exhibit Lampland's changes, they leave it uncertain whether these changes are due to motion or to alterations in the relative brightness. Baade has recently photographed the Crab nebula at the 100-inch telescope, using red-sensitive plates, which record beautifully definite details in the structure and which will be invaluable for future studies of the expansion. On his photographs there appears a bright nucleus about 8″ preceding and 2″ north of the origin of co-ordinates. If this is the true center from which the nebula originated, it has, according to the present investigation, a proper motion $\Delta x = -0''.037$, $\Delta y = +0.005$, per year. It is tempting to imagine that this red nucleus, although unobtrusive on the photographs, emits the radiation necessary to keep the Crab nebula luminous but mostly of so small a wave length that it is stopped by the earth's atmosphere.

[2] *Pub. A.S.P.*, **33**, 79, 1921.

The mean of the two values of t, 766 years, indicates—with considerable uncertainty—the year A.D. 1172 as the date of the outburst.

Mayall's estimate[3] of the distance of the Crab nebula, based on his value 1300 km/sec of the maximum radial velocity of expansion, together with my results of 1921, seems to need but little correction. On the assumption that this velocity corresponds to a point $2'.7$ from the radiant, where the image of the nebula becomes faint and where, according to the present study, the angular displacement is $0''.21$ per year, the distance of the nebula appears to be 1300 parsecs, or 4200 light-years. At this distance the proper motion of the nucleus, found above, denotes a velocity across the line of sight of about 230 km/sec, and the greatest diameter of the nebula comes out about 6 light-years.

CARNEGIE INSTITUTION OF WASHINGTON
MOUNT WILSON OBSERVATORY
February 1939

[3] *Ibid.*, **49**, 103, 1937.

PROMINENCES AND THE SUNSPOT CYCLE

VINICIO BAROCAS

ABSTRACT

The investigations by Lockyer, Evershed, and Bocchino on the relation between prominences and spots are extended to all the prominence observations from 1880 to 1937. A diagram is traced of all the six cycles under consideration, and the behavior of high- and low-latitude prominences and their relationship to the sunspot cycle is examined.

The so-called "metallic prominences" are present only in the low-latitude zone.

The problem concerning the distribution of prominences on the solar disk has interested many astronomers. G. Bocchino in a recent publication[1] has continued the works of Lockyer and Evershed and has extended the search from 1880 to 1931, about five cycles. She has studied the migration of prominences during the sunspot cycle, bringing out new characteristics of the latitude and of the frequency of the prominences.

The material already available from the foregoing five cycles extended up to 1937 now can be discussed in order to contribute to the knowledge of the two zones of prominences (high- and low-latitude) and their behavior in connection with the eleven-year cycle.

Evershed[2] has already shown that prominences can be divided into two different types: low- and high-latitude prominences. The difficulty, however, was to determine the latitude which separates them. In the Evershed diagrams there is a large zone between them, but it is so wide that it is impossible to determine a value for the limiting latitude. Usually, the observers who have worked on this problem have taken the mean width of the above-mentioned zone. We have chosen the value of $\pm$ 40° as the separation between high and low prominences. Then we will call "high-latitude" prominences those which have a latitude greater than 40° and "low-latitude" prominences those under 40°.

We can trace a diagram, as was done by Bocchino,[3] for the years

[1] *Pub. Arcetri*, No. 51, p. 7, 1933.

[2] *Mem. Kodaikanal Obs.*, **1**, ii, 1917.

[3] See also G. Abetti, *The Sun*, p. 156, London, 1938.

1880–1937, taking the years as abscissas and the latitudes of the greatest activity as ordinates. These latitudes are determined by bisecting the diagram of mean areas at 40° and taking the weighted mean of each part.

The values of prominence areas are taken from Bocchino's publication and the Arcetri's observations.[4]

For the low-latitude prominences we write

$$\frac{2.5 \times A + 7.5 \times B + \ldots + 37.5 \times Z}{2.5 + 7.5 + \ldots + 37.5},$$

where 2.5, etc., is the mean latitude, and A, B, etc., are the mean areas of the prominences; these apply also to the high-latitude prominences.

Table 1 gives the mean values for both the northern and the southern hemisphere. The value in the column "Spots" is taken for each year from the *Monthly Notices*. From this table the diagram in Figure 1 has been traced; it confirms Lockyer's and Evershed's deductions.

Let us now analyze the curve of low-latitude prominences in the diagram. It follows the spot development very closely, although it is limited to a zone between ± 18° and ± 28°, while the spots are found, as is well known, in a zone between ± 7° and ± 23°.

Prominences appear at a distance of 10° north and south from the spots and follow them, but with a smaller range of latitude. At the minimum period of the sunspot cycle the latitude of the low-latitude prominences and spots is a maximum. The minimum latitude for prominences and spots is reached one or two years before sunspot minimum. Yet this law is not a rigid one; it is sufficient to observe that, when spots reach their minimum of latitude, the prominences of low latitude, while continuing their motion, are moving toward higher latitudes after attaining the minimum just referred to. During the period when the spots reach their lowest latitudes, we have the greatest distance in latitude between spots and low-latitude prominences.

The determination of the correlation coefficient will confirm what

[4] *Pub. Arcetri*, Nos. 52–56, 1934–1938.

has been said about the analogy which exists between the curves of the low-latitude prominences and of the spots. Mineur's method has been followed in this investigation, and from Figure 2 it is found that the correlation coefficient is about 1 ($\cos \sigma = 0.99$). In Figure 2 the two straight lines start from above 10° on the abscissa for, as is clearly

TABLE 1

Years	Low Lat.	High Lat.	Spots	Years	Low Lat.	High Lat.	Spots
1880	25°.5	54°.1	19°.7	1909	20°.7	49°.0	9°.7
1881	23.8	57.9	18.2	1910	19.0	52.7	9.9
1882	22.3	64.8	17.6	1911	23.3	52.6	6.9
1883	22.3	54.8	12.4	1912	22.0	49.8	14.1
1884	19.8	55.7	11.2	1913	28.4	49.4	22.4
1885	21.4	50.4	11.5	1914	26.8	49.8	22.1
1886	20.0	48.8	10.4	1915	26.4	53.8	18.8
1887	21.5	50.8	8.5	1916	23.9	58.7	16.0
1888	23.0	51.2	7.3	1917	21.3	61.1	14.2
1889	24.4	50.2	9.6	1918	20.4	59.9	12.8
1890	27.8	48.5	22.0	1919	19.7	48.3	10.3
1891	25.3	52.8	20.2	1920	19.9	46.9	10.6
1892	25.7	56.2	18.4	1921	21.4	49.5	8.1
1893	23.1	56.4	14.6	1922	22.6	49.3	7.7
1894	22.2	59.4	13.9	1923	23.7	53.1	15.6
1895	20.8	48.0	13.4	1924	26.8	54.3	23.9
1896	24.5	48.6	14.2	1925	24.9	56.6	20.0
1897	18.7	52.9	8.0	1926	23.4	62.1	18.6
1898	20.4	50.6	10.3	1927	21.3	61.8	11.6
1899	21.8	49.9	8.3	1928	21.5	59.0	13.6
1900	20.7	52.0	7.5	1929	20.9	53.4	10.5
1901	20.2	53.4	12.4	1930	20.9	50.6	9.8
1902	25.6	53.3	17.0	1931	20.2	48.6	8.6
1903	26.0	53.5	12.6	1932	22.0	50.6	8.4
1904	23.5	56.7	16.6	1933	27.3	47.7	9.5
1905	22.1	57.0	13.6	1934	26.7	48.6	22.3
1906	22.2	63.2	14.0	1935	25.6	50.8	23.1
1907	22.1	54.5	12.0	1936	23.0	57.2	28.2
1908	19.8	52.1	11.9	1937	21.4	63.1	.....

seen by the dispersion of the points between 6° and 10°, if their mean is taken, there will be two perpendicular lines, i.e., a correlation coefficient of 0, the angle σ being 90° ($\cos \sigma = 0$).

Let us now see what the meaning of this result is. A correlation of form undoubtedly exists between the two diagrams under discussion; but it is almost zero for the smallest value of latitude that can be deduced from what has been said, and particularly by considering the years 1888, 1911, 1922, and 1932 in Figure 1.

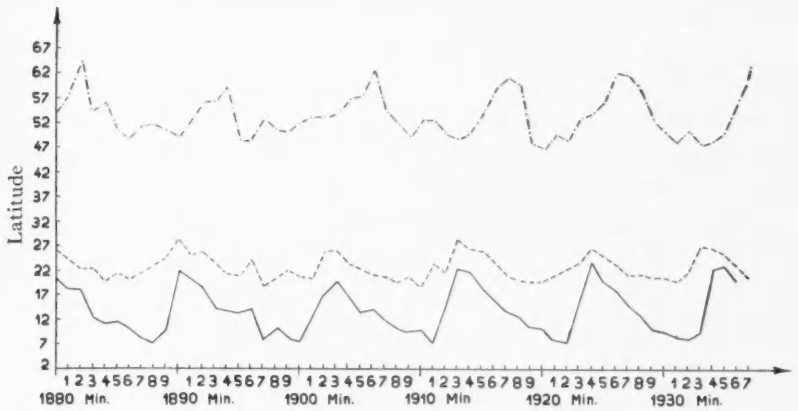

FIG. 1

- - - - low-latitude } prominences
- - - · high-latitude }
—— spots

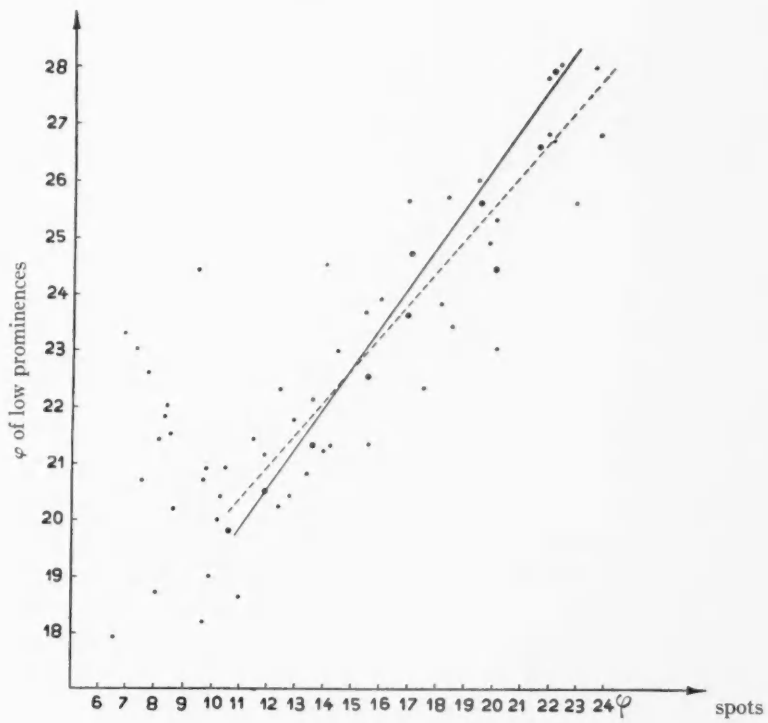

FIG. 2

Turning now to the diagram of the high-latitude prominence, we see that it is more difficult to find an analogy between this curve and that of the spots. Prominences drift toward higher latitudes and reach them about the time of sunspot maximum. Then, while the high-latitude prominences are, in a given year, at their highest latitudes, low-latitude prominences in the same year reach their lowest latitudes. The low-latitude prominences attain the highest latitudes

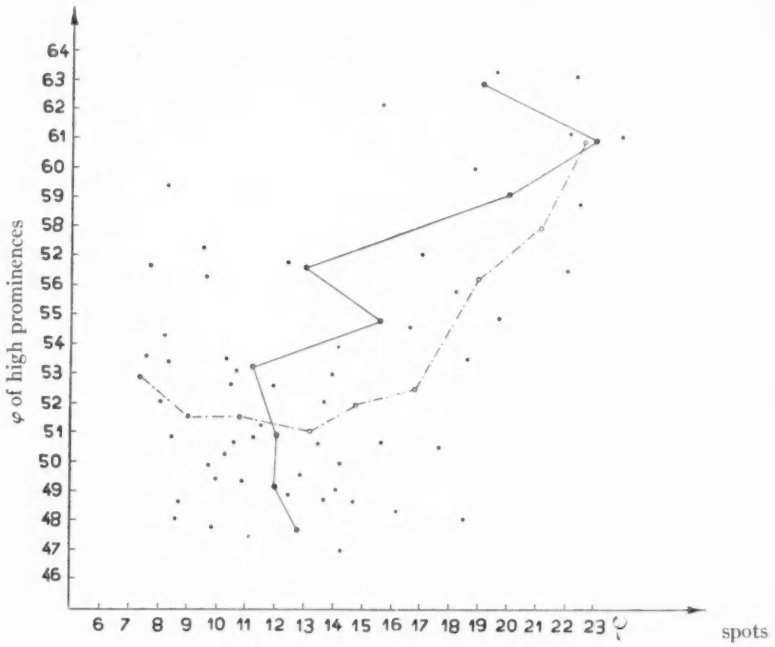

FIG. 3

when the high-latitude prominences are at a minimum. It is rather difficult in this case to find the correlation coefficient, since the two diagrams are not in phase. A remarkable result is obtained by displacing the diagrams of the high-latitude prominence by three years with reference to that of the spots. This gives an almost perfect coincidence between the maxima, but the minima are unaffected by the displacement: the minima of the prominences precede those of the spots. The dispersion of the points in Figure 3 shows that there is no correlation in form between the two curves under considera-

tion. The two lines are almost perpendicular in low latitudes, and they form a small angle in high latitudes; in the first part there is no correlation; in the second one should naturally exist, but it is a forced correlation, for the curve has been displaced in order to obtain the coincidence of maxima. It can therefore be stated that a correlation does not exist between the curve of the high-latitude prominences and that of the spots, or at least only as far as it concerns the duration of the cycle.

In Figure 1 we see that the migration of high-latitude prominences toward the poles is not connected with the phenomena of the low-latitude prominences. Yet they reach a maximum latitude when the spots and the low-latitude prominences drift toward the equator, that is to say, some years after the spots and the low-latitude prominences have reached their maximum latitude. This fact occurs, as is well known, about the period of sunspot maximum. During the maximum of the cycle we have, then, a greatly disturbed zone of low latitude at a mean latitude of about $\pm 20^\circ$, while at the high-latitude zone the prominences are at their maximum latitude of about 60° and are already decreasing in activity.

During the period of sunspot minimum the low-latitude prominences also appear at their highest latitudes; this fact may be attributed to the presence of two zones of activity. By a careful study of these prominences and of dark flocculi a distinction can be made between the prominences of the old and the new cycles; at present, except for the latitude, there is no criterion by which we can make this distinction. In the case of the spots, the sign of the magnetic field provides a definite distinction.

The present investigation may also explain why at the minimum period there are two zones of activity at low latitudes and only one at high latitudes.

To give a general view of the phenomenon, another diagram (Fig. 4) has been drawn in which the abscissas represent years and the ordinates represent the mean areas expressed in prominence units.

The curves representing the motion of the prominences (low- and high-latitude) are the means for the northern and southern hemispheres for the six cycles from 1880 to 1937.[5] The ordinates of the

[5] Values taken from various issues of *Pub. Arcetri*.

curve for the spots are Wolf numbers taken from the Zurich publications. In Table 2, their values are given. The prominences are divided, as before, into low- and high-latitude prominences.

Analyzing Figure 4, it will be noted that in this diagram the low-latitude prominences follow the spots, i.e., they follow the spots not only in the latitude distribution but also in frequency. High-latitude prominences, on the contrary, behave in a different manner: they

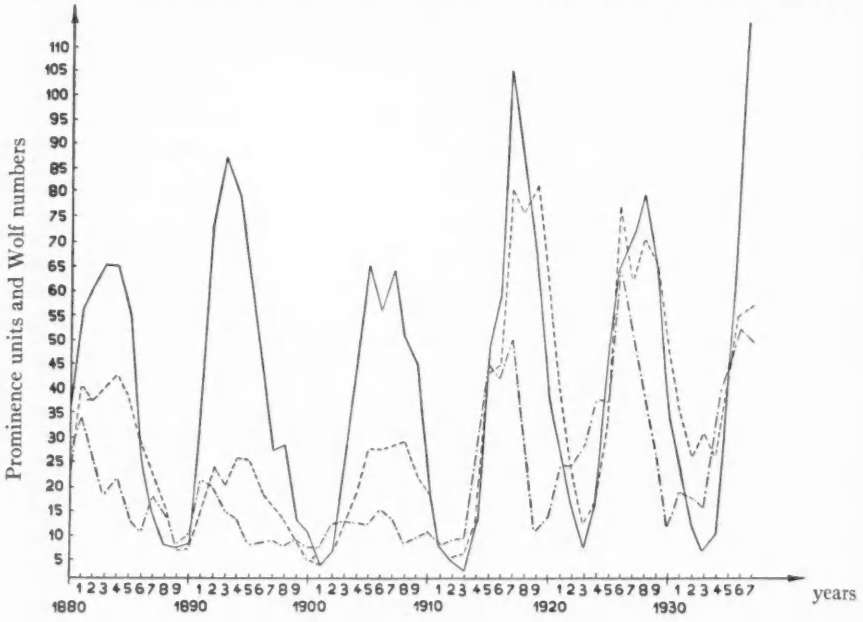

FIG. 4

- - - - low-latitude
- - - - high-latitude } prominences
—— spots

reach a maximum about two years before the maximum of the sunspot cycle.

To give a clear idea of the phenomenon, the diagram in Figure 5 shows the curves representing the means of the six cycles given in Figure 4 for spots and for high- and low-latitude prominences. In Figure 5 the abscissas represent the years of the cycle and the ordinates represent the mean value given in Table 3, expressed in prominence units.

The first thing to be observed in Figure 5 is that the curve for the spots reaches its maximum in the fifth year.

High-latitude prominences reach a maximum two years before the spots and then decrease to a minimum five years before the spots; they have, therefore, no connection with the spots. But the cycle

TABLE 2

Years	Low Lat.	High Lat.	Wolf No.	Years	Low Lat.	High Lat.	Wolf No.
1880	201.2	262.9	32.3	1909	217.2	82.5	43.9
1881	393.1	334.5	54.3	1910	177.3	96.6	18.6
1882	366.5	238.8	59.7	1911	76.1	64.3	5.7
1883	387.2	174.0	63.7	1912	42.8	77.0	3.6
1884	420.5	206.3	63.5	1913	46.0	78.1	1.4
1885	372.2	124.0	52.2	1914	121.5	260.0	9.6
1886	275.3	91.4	25.4	1915	415.7	431.0	47.4
1887	219.8	168.7	13.1	1916	434.2	408.5	57.1
1888	152.3	131.7	6.8	1917	791.8	486.9	103.9
1889	54.0	69.0	6.3	1918	743.7	275.7	80.6
1890	58.4	88.4	7.1	1919	797.6	93.7	63.6
1891	132.3	204.7	35.6	1920	607.0	123.8	37.6
1892	229.7	189.0	73.0	1921	378.7	233.6	26.1
1893	190.5	139.9	84.9	1922	210.5	229.1	14.2
1894	244.1	122.4	78.0	1923	114.9	274.9	5.8
1895	239.4	67.0	64.0	1924	157.5	364.9	16.7
1896	179.6	70.7	41.8	1925	315.1	360.4	44.3
1897	151.9	77.1	26.2	1926	755.6	627.1	63.9
1898	120.3	67.4	26.7	1927	599.5	517.8	69.0
1899	73.3	77.8	12.1	1928	693.6	363.5	77.8
1900	38.5	64.0	9.5	1929	643.0	252.2	65.0
1901	29.0	63.2	2.7	1930	470.7	100.2	35.7
1902	49.4	111.8	5.0	1931	335.7	175.6	21.2
1903	115.5	117.1	24.4	1932	249.0	164.5	11.1
1904	164.0	113.9	42.0	1933	294.5	142.0	5.7
1905	263.7	111.1	63.5	1934	248.5	306.5	8.7
1906	261.5	140.9	53.8	1935	388.0	425.5	36.1
1907	270.8	124.8	62.0	1936	531.5	506.0	80.4
1908	277.5	73.5	48.5	1937	556.6	486.3	114.4

of the high-latitude prominences also lasts eleven years, although it is not in phase with the spot cycle. Its maximum appears in the eighth year, if we take the minimum of the curve as the beginning of the cycle, as in the case of the spots.

More interesting is the curve of low-latitude prominences, which behave differently. They, too, reach a maximum two years before the spots, but afterward they decrease and reach a secondary minimum one year before sunspot maximum. Then they increase and

attain another maximum, higher than the preceding, at the same time that the spots do. The minimum occurs in the same year as that of the spots. The curve of the low-latitude prominences follows

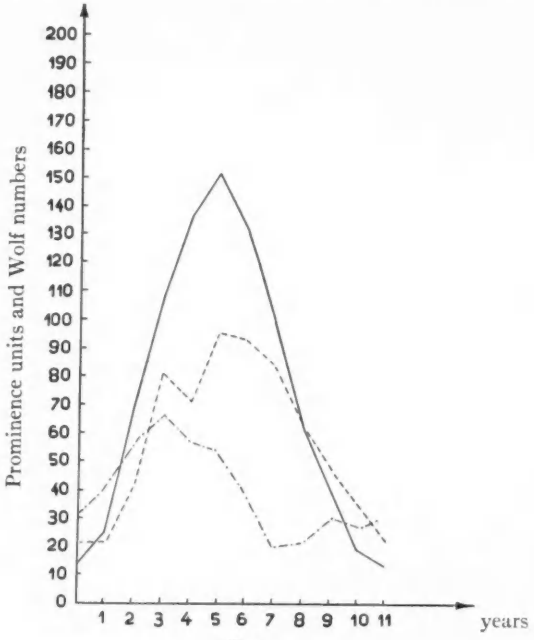

FIG. 5

TABLE 3

Spots	Low Lat.	High Lat.	Spots	Low Lat.	High Lat.
14.2	21.2	31.2	131.8	92.0	38.0
25.6	21.4	41.4	99.4	83.6	19.8
69.6	41.0	56.5	62.4	63.4	21.0
108.4	81.0	66.8	41.2	46.8	29.6
136.4	71.8	56.8	19.6	34.0	26.2
152.2	94.0	53.0	13.2	21.0	30.4

very nearly that of the spots with respect to its maximum, its minimum, and its amplitude, except for its behavior in the third year before sunspot maximum.

From Figure 5 we see that during the period of sunspot minimum the low-latitude prominences also have a minimum while the high-latitude prominences are already advanced in their cycle. At the beginning of the spot cycle the three curves increase rapidly; and the high- and low-latitude prominences reach a maximum in the same year, exactly two years before the spot-cycle maximum. The high-latitude prominences then begin to decrease and are followed by the low-latitude prominences. One year before the spot-cycle maximum the activity of the spots, which has reached a very high value, begins to make itself felt in the low-latitude prominences, and the latter suddenly increase and reach a maximum at the same time as the spots; then they follow the behavior of the spots, up to their respective minima.

The high-latitude prominences, after the secondary minimum of the low-latitude prominences, slowly decrease; but from the time of maximum activity they hasten toward their minimum.

It has been shown by G. Abetti[6] that the shape of the corona depends upon the development and the frequency of the prominences in high latitudes.

Having distinguished between high- and low-latitude prominences, it is interesting to investigate the difference in their constitution. Several observers have classed them as metallic and hydrogenous prominences according to their spectra, because in the former many metallic lines are present, while in the latter only hydrogen lines appear.

The Kodaikanal Observatory publishes twice a year a list of the metallic prominences, with their positions, their height, and the origin of their lines. The metallic prominences usually differ from the others by the presence of b_1, b_2, and b_4 of *Mg;* D_1, and D_2 of *Na;* and a group of lines of *Fe* I, *Fe* II, *He*, and *Cr*. I have examined these lists from 1912 to the first half of 1938 and have noticed that the prominences present more or less the same lines, i.e., those given in Table 4. Several prominences show numerous lines of other elements; but if we take their height, we find that they are so low that they may be regarded as more like the chromosphere itself than as

[6] *Ibid.*, No. 56, p. 53, 1938, and *Mem. Soc. Astr. It.*, **9**, 161, 1938.

prominences, and this probably explains the presence of lines that are not usually found in prominences. We define "prominences" as all eruptions that attain a height of 20″ (about 14,000 km—the height in the chromosphere of *Ca* II) or more.

The latitude at which metallic prominences appear is what we

TABLE 4*

Chromosphere	Elements	I_d	I_f	Height	E.P.
4923.9	*Fe* II	5	30	2000	2.88
5015.6	*He*	.....	2	2500	20.52
5018.4	*Fe* II	4	25	2000	2.88
5167.3	*Mg*	15	18	1500	2.70
5167.5	*Fe*	5	18	1500	1.48
5168.9	*Fe*	7	25	1500	2.88
5171.6	*Fe*	7	25	1500	2.88
5172.6	*Mg*	20	30	2000	2.70
5183.6	*Mg*	30	40	2500	2.70
5197.7	*Fe* II	2	12	500	3.22
5204.8	*Cr-Fe*	8	7	500	0.94
5206.2	*Cr*	5	8	600	0.94
5208.4	*Cr*	5	12	600	0.94
5227.0	*Fe-Cr*	8	8	500	1.55
5234.6	*Fe* II	2	15	500	3.21
5269.5	*Fe*	8	15	600	0.86
5270.6	*Fe-Ca*	7	7	500	1.60
5275.9	*Fe* II	6	20	500	3.19
5284.1	*Fe* II	1	8	400	2.88
5316.6	*Fe* II	6	30	850	3.14
5324.2	*Fe*	7	7	400	3.20
5362.8	*Fe* II	3	15	500	3.19
5383.3	*Fe*	6	6	400	.....
5889.9	*Na*	30	25	1500	0.00
5895.9	*Na*	20	20	1500	0.00
6678.1	*He-Fe*	5	20	2200	21.13
7065.2	*He*	.....	6	1000	20.87

* I_d = intensity on the disk; I_f = intensity in the flash.

have called "low latitude," i.e., less than 40°. Table 5 gives a list of the metallic prominences in high latitudes observed in the period 1912–1938. We find that during a period of 26.5 years, out of 835 metallic prominences observed on the sun, only 28, or 3 per cent, were in high latitudes; and all showed the same lines, namely, b_1, b_2, b_4, D_1, and D_2.

When we take all prominences, irrespective of whether their spectra show metallic or hydrogen lines, the percentage of high-latitude prominences is 41.

TABLE 5*

Date	No. of Met. Prom.	Lat.	Height	Elements
1912	10			
Mar. 19		52°.0 S.	45″	*Na–Mg–Fe*
Sept. 31		78.5 N.	20	*Na–Mg–Fe*
1913	4			
Mar. 13		46.5 S.	25	*Na–Mg–Fe*
Mar. 26		44.5 S.	70	*Na–Mg–Fe–He*
Mar. 26		41.5 S.	25	*Na–Mg–Fe–He*
1914	12			
April 6		45.0 S.	65	*Mg–Fe*
Oct. 11		49.5 S.	65	*Na–Mg–Fe–Fe* II
Nov. 4		50.0 N.	60	*Na*
Nov. 26		52.0 N.	20	*Na–Mg–Fe*
1915	37			
Jan. 15		53.0 N.	40	*Na–Mg–Fe*
May 20		51.5 S.	30	*Na–Mg–Fe*
1916	42			
Jan. 25		42.0 S.	60	*Na–Mg–Fe–Fe* II
Dec. 10		43.0 S.	30	*Na–Mg–Fe–Fe* II
Dec. 25		41.0 S.	40	*Na–Mg–Fe–Fe* II
1917	46	.....	.....	.....
1918	51	.....	.....	.....
1919	112			
Jan. 28		41.0 S.	70	*Na–Mg–Fe–Fe* II
Feb. 23		43.0 N.	55	*Na–Mg–Fe–Fe* II
Mar. 2		55.5 S.	25	*Na–Mg–Fe–Fe* II–*Cr*
Mar. 2		45.5 S.	50	*Na–Mg–Fe–Fe* II–*Cr*
1920	110			
Jan. 12		52.0 N.	50	*Na–Mg–Fe*
Jan. 17		46.0 N.	40	*Na–Mg–Fe*
Feb. 5		42.5 N.	50	*Na–Mg–Fe*
Nov. 30		42.5 N.	70	*Na–Mg–Fe*
Dec. 3		41.0 N.	75	*Na–Mg–Cr–Fe* II
Dec. 12		72.0 N.	110	*Na–Mg–Fe*
1921	42	.....	.....	.....
1922	31	.....	.....	.....
1923	6	.....	.....	.....
1924	6	.....	.....	.....
1925	30	.....	.....	.....
1926	68			
Feb. 16		41.0 N.	50	*Na–Mg–Fe–He–Fe* II
Feb. 17		46.5 N.	35	*Na–Mg–Fe*
1927	56			
Mar. 24		42.5 N.	20	*Na–Mg–Fe–He–Fe* II
1928	22	.....	.....	.....
1929	46	.....	.....	.....
1930	13			
Dec. 26		45.0 N.	30	*Na–Mg–Fe*
1931	9	.....	.....	.....
1932	1	.....	.....	.....
1933	1	.....	.....	.....
1934	4	.....	.....	.....
1935	11	.....	.....	.....
1936	27	.....	.....	.....
1937	24	.....	.....	.....
1938	14	.....	.....	.....

* The second column gives the number of the metallic prominences for the year. Values for 1938 are limited to the first half-year.

The difference between eruptive and quiescent prominences is perhaps only a difference in intensity; Pettit has shown that the spectra of quiescent prominences contain lines with an intensity greater than 30 on Mitchell's scale, while the intensity of the faint lines of the metallic prominences is 15 on the same scale.

The Kodaikanal observations in the region between 4923.9 A and 7065 A show eleven lines in the metallic prominences fainter than 15 in Mitchell's scale (see Table 4); these lines include those of *Cr*, *Fe*, and *Ca*. The three lines of ionized barium which have intensities of 25, 20, and 20 do not appear.

What has been said about the metallic prominences observed between 1912 and the present time agrees with Pettit's examination[7] of the plate of the eclipse of June 8, 1918, with the exception of some lines fainter than 15 observed at Kodaikanal. In Table 4, I_d is the intensity on the disk and I_f in the flash, according to Mitchell.

Whether the differences in the spectra of both types of prominences depend only upon the intensities of the lines could only be decided after a systematic study of the spectra of prominences photographed by Lyot's method. The eruptions are certainly more violent at low latitudes, where the excitation of the elements in the chromosphere and prominences must be greater than in the high-latitude zones.

R. Observatory Arcetri-Firenze
November 1938

[7] *Mt. Wilson Contr.*, No. 451, p. 2; *Ap. J.*, **76**, 9, 1932.

THE POINT-SOURCE MODEL WITH CONSTANT OPACITY

PHILIP C. KEENAN

ABSTRACT

The differential equations for the point-source model, in the form derived by Chandrasekhar and von Neumann, have been integrated numerically for eight values $M\mu^2$ ranging from 19.3 to 31,500 in units of the sun's mass. All the solutions are characterized by negative density gradients in the central region, since ρ becomes zero at the center. The radius at which the density is a maximum shifts outward with increasing mass so that ξ^*, the fraction of the radius containing 90 per cent of the total mass, increases steadily from 0.65 to 0.98. For large masses the central regions are practically isothermal.

The mass-luminosity curve becomes less steep with increasing mass, approaching the line $L \sim M$.

The physical interest of the point-source model is increased by the agreement found between the model and the massive Trumpler stars, both in the values of ξ^* for corresponding masses and in position in the mass-luminosity diagram.

The stellar model with the sources of energy concentrated effectively at the center forms an important limiting case and was considered first by Eddington,[1] who obtained a numerical solution for one set of values for M, L, R, and μ. Further discussions have been given by Cowling,[2] Milne,[3] Strömgren,[4] and Biermann,[5] but the most complete development of the general properties of such models is due to Chandrasekhar and von Neumann.[6]

Among the point-source models, those with constant opacity (κ) provide a set of limiting configurations in so far as at very high temperature the main source of opacity arises from electron scattering (for electron scattering κ = const.). The complete discussion of such models requires considerable care, for, if we start with the assumption of radiative equilibrium at the surface and continue inward, a stage will be reached where the radiative gradient will exceed the adiabatic gradient. Here the radiative gradient will become unstable, and it is generally assumed that beyond this point the

[1] *M.N.*, **85**, 408, 1925; *The Internal Constitution of the Stars*, p. 124, 1926.

[2] *M.N.*, **91**, 92, 1930.

[3] *M.N.*, **91**, 4, 1930.

[4] *Zs. f. Ap.*, **2**, 345, 1931.

[5] *Zs. f. Ap.*, **3**, 116, 1931; *ibid.*, **4**, 61, 1932.

[6] S. Chandrasekhar, *An Introduction to the Study of Stellar Structure*, chap. ix, p. 332, 1939.

adiabatic temperature gradient will be set up. Although a rigorous discussion has been given only for the case where the radiation pressure as a factor in hydrostatic equilibrium is negligible,[6] there can be no doubt that a continuation of the equations beyond the region of known stability requires caution. In spite of this, the establishment of the (L, M, κ, μ) — relation in detail for the complete point-source model is of particular value in that it should provide a "minimal case."

In view of these considerations, numerical integrations have been carried out for the complete point-source model with κ constant, in which the mass of the star has been exactly used up when the center has been reached. No attempt has been made to deal with models with point mass at the center.

The equations of equilibrium,

$$\frac{d(p_g + p_r)}{dr} = -\frac{GM(r)}{r^2}\rho$$

and

$$\frac{dp_r}{dr} = -\frac{\kappa L}{4\pi c r^2}\rho ,$$

are transformed by the substitutions:[7]

$$r = a\xi = \frac{a}{x} ; \qquad P_g = \Pi z ; \qquad P_r = \Pi_r t ,$$

where the constants are connected by the relations

$$a = \left[\frac{\kappa L}{16\pi^2 cG}\frac{k}{\mu H}\left(\frac{3}{a}\right)^{1/4}\right]^{1/3}\Pi_r^{-1/4}$$

$$\Pi = \left[\frac{4\pi c^2}{\kappa^2 L^2 G}\left(\frac{k}{\mu H}\right)^4\frac{3}{a}\right]^{1/3}\Pi_r$$

into the forms

$$\frac{dx}{dt} = -z^{-1}t^{1/4} \qquad \text{(I)}$$

[7] Cf. *ibid.*, for notation and derivation of equations I and II.

and

$$\frac{d^2z}{dt^2} = -x^{-4} \qquad \text{(II)}\,.$$

For the case under consideration the three necessary boundary conditions are:

a) At the surface, where $t = 0$, $\quad z = 0$.

b) At the surface, where $t = 0$, $\quad \frac{dz}{dt} = \delta_1 > 0$.

c) At the center, where $t = t_c$, $\quad M_{r=0} = 0$.

Furthermore, since equations I and II admit of a constant of homology so that the equations are invariant to the transformation

$$x, z, t \rightarrow C^{1/4}x, Cz, Ct$$

where C is an arbitrary real number, we can normalize the units of x so as to make $x = 1$ for $t = 0$.

It is shown in Chandrasekhar's discussion[6] that the solutions satisfying these boundary conditions are those for which the zt-curve passes through a maximum and intersects the t-axis at t_c with a slope $(dz/dt)_c = -\delta_2$. The mass and luminosity relations for these models are

$$M = 1.117 \odot \delta_2^{1/2}(\delta_1 + \delta_2)\mu^{-2}$$

$$L = \frac{4\pi cGM}{\kappa}\frac{\delta_1}{\delta_1 + \delta_2} = 1.471 \times 10^4 \kappa^{-1}\mu^{-2}\delta_2^{3/2}\,.$$

The constant δ_2 is uniquely determined by δ_1, and it can be shown that for a sufficiently large positive value of δ_1, δ_2 must be positive. As δ_1 decreases, δ_2 also diminishes, and for a critical positive value $(\delta_1)_0$, δ_2 becomes equal to zero, corresponding to a model of zero mass.

The general procedure in carrying out each solution is to start at the surface with some value of δ_1, presumably greater than the as yet unknown $(\delta_1)_0$, and to integrate inward until $z = 0$, where t_c and δ_2 are then found. At this point $r = 0$, and, hence, x goes to infinity. As δ_1 approaches the critical value, the range of integration becomes greater and the numerical work becomes increasingly difficult, but this is

not serious, since we are primarily interested in models of large mass (large δ_1), for which no solutions have been attempted previously.

In the actual numerical work it is convenient to introduce new variables τ and ζ defined[8] by

$$t = \delta_1 \tau \; ; \qquad z = \delta_{15}^2 \zeta \; .$$

Then I and II become

$$\frac{dx}{d\tau} = \delta_1^{-3/4} \zeta^{-1} \tau^{-1/4} \qquad \text{(I')}$$

$$\frac{d^2\zeta}{d\tau^2} = - \, x^{-4} \qquad \text{(II')}$$

and the initial conditions at the surface of the star are now:

$$At \; \tau = 0 \; ; \qquad x = 1 \, , \qquad \zeta = 0 \, , \qquad \frac{d\zeta}{d\tau} = 1 \, .$$

Since $dx/d\tau$ is infinite at the boundary, it is necessary to obtain series expansions to start the solutions. Thus, for x and ζ near $\tau = 0$ we find by repeated substitution and integration:

$$\begin{aligned} x = 1 &+ \delta_1^{-3/4}\left(4\tau^{1/4} + \tfrac{2}{5}\tau^{-5/4} + \tfrac{1}{9}\tau^{9/4} + \tfrac{1}{26}\tau^{13/4} + \ldots .\right) \\ &- \delta_1^{-3/2}\left(\tfrac{512}{135}\tau^{3/2} + \tfrac{3328}{2725}\tau^{5/2} + \tfrac{404,352}{904,981}\tau^{7/2} + \ldots .\right) \\ &+ \delta_1^{-9/4}\left(\tfrac{512}{21}\tau^{7/4} + \tfrac{133,072}{10,125}\tau^{5/2} + \tfrac{10,496}{1155}\tau^{11/4} + \ldots .\right) \\ &\mp \ldots . \, , \end{aligned}$$

$$\begin{aligned} \zeta = \tau - \frac{\tau^2}{2} &+ \delta_1^{-3/4}\left(\tfrac{256}{45}\tau^{9/4} + \tfrac{128}{585}\tau^{13/4} + \tfrac{64}{1989}\tau^{17/4} + \ldots .\right) \\ &- \delta_1^{-3/2}\left(\tfrac{128}{3}\tau^{5/2} + \tfrac{25,472}{4725}\tau^{7/2} + \tau^{9/2} + \ldots .\right) \\ &+ \delta_1^{-9/4}\left(\tfrac{20,480}{77}\tau^{11/4} + \tfrac{35,604,480}{467,775}\tau^{15/4} + \ldots .\right) \\ &\mp \ldots . \end{aligned}$$

For small masses the series converge slowly, and it was found more convenient to extend the first one or two values by Kutta's modifica-

[8] For the suggestion of this transformation I am indebted to Professor Walter Bartky.

tion of Simpson's rule to the point where ordinary forward integration could be begun, than to work with extremely small intervals in τ.[9]

Solutions were made for eight values of δ_1, corresponding to a range of 19.3 to 31,500 in $M\mu^2$, where M is expressed in units of the sun's mass. From a plot of δ_2 against the corresponding values of $\delta_1 + \delta_2$, it was then possible to estimate that the critical value $(\delta_1)_0$, for which $\delta_2 = 0$, is approximately 8.

In preparing Table 1, which gives the results for the individual models, the solutions have been condensed considerably, particularly in the case $\delta_1 = 11.51$, for which the original integration required 229 steps. The second column of the table lists the temperature ex-

TABLE 1

$\delta_1 = 625$ $M\mu^2 = 31{,}500$ $\tau_c^{1/4} = 1.225$ $(\zeta/\tau^{1/4})_{max} = 1.019$			$\delta_1 = 107.3$ $M\mu^2 = 1954$ $\tau_c^{1/4} = 1.3420$ $(\zeta/\tau^{1/4})_{max} = 0.6650$		
$r/R = 1/x$	T/T_c	ρ/ρ_{max}	$r/R = 1/x$	T/T_c	ρ/ρ_{max}
0.990	0.258	0.050	0.963	0.236	0.047
.985	.386	.190	.946	.352	0.156
.982	.459	.311	.936	.419	0.256
.979	.546	.498	.924	.498	0.414
.976	.604	.640	.910	.593	0.640
.974	.649	.752	.900	.656	0.796
.972	.686	.838	.891	.705	0.901
.971	.718	.906	.884	.745	0.966
.969	.747	.953	.877	.780	0.996
.968	.772	.983	.873	.796	1.000
.966	.795	.997	.870	.811	0.996
.965	.816	.998	.863	.838	0.970
.964	.836	.986	.848	.886	0.846
.962	.854	.960	.831	.928	0.640
.961	.872	.920	.807	.964	0.365
.959	.888	.870	.786	.981	0.206
.958	.903	.809	.769	.989	0.122
.956	.918	.736	0.730	0.997	0.036
.954	.932	.653			
.952	.946	.558			
.949	.958	.454			
.946	.971	.340			
.941	.983	.218			
0.932	0.994	0.087			

[9] Cf. Levy and Baggott, *Numerical Studies in Differential Equations*, I, 106, 1934. The forward integration was done by their Method III of chap. iv. See also pp. 159–60.

TABLE 1—*Continued*

$\delta_1 = 73.1$ $\tau_c^{1/4} = 1.4013$	$M\mu^2 = 1020$ $(\zeta/\tau^{1/4})_{max} = 0.7295$		$\delta_1 = 54.3$ $\tau_c^{1/4} = 1.466$	$M\mu^2 = 600$ $(\zeta/\tau^{1/4})_{max} = 0.806$	
$r/R = 1/x$	T/T_c	ρ/ρ_{max}	$r/R = 1/x$	T/T_c	ρ/ρ_{max}
0.952	0.226	0.043	0.940	0.216	0.039
.929	0.338	0.142	.913	.323	0.129
.917	0.401	0.234	.898	.384	0.212
.902	0.477	0.379	.880	.456	0.345
.884	0.568	0.592	.859	.542	0.542
.871	0.628	0.744	.844	.600	0.687
.861	0.675	0.852	.833	.645	0.796
.852	0.714	0.928	.822	.682	0.878
.836	0.776	0.998	.805	.742	0.974
.828	0.803	1.000	.789	.790	1.000
.821	0.827	0.982	.774	.831	0.968
.813	0.849	0.946	.758	.866	0.888
.805	0.870	0.894	.741	.898	0.769
.797	0.888	0.827	.722	.926	0.617
.779	0.923	0.653	.698	.952	0.435
.755	0.954	0.434	.683	.965	0.336
.738	0.969	0.309	.663	.976	0.231
.714	0.983	0.177	.632	.988	0.123
.694	0.990	0.109	0.152	0.999	0.012
.656	0.996	0.039			
0.135:	1.000	0.004			

$\delta_1 = 42.6$ $\tau_c^{1/4} = 1.537$	$M\mu^2 = 383$ $(\zeta/\tau^{1/4})_{max} = 0.891$		$\delta_1 = 29.0$ $\tau_c^{1/4} = 1.702$	$M\mu^2 = 184$ $(\zeta/\tau^{1/4})_{max} = 1.1025$	
$r/R = 1/x$	T/T_c	ρ/ρ_{max}	$r/R = 1/x$	T/T_c	ρ/ρ_{max}
0.929	0.206	0.004	0.908	0.186	0.029
.898	.308	.019	.868	.278	.094
.880	.366	.193	.846	.330	.156
.860	.435	.314	.822	.393	.256
.836	.517	.496	.793	.467	.409
.820	.573	.633	.774	.517	.528
.806	.615	.741	.759	.556	.626
.796	.651	.824	.747	.588	.706
.777	.708	.936	.726	.639	.829
.760	.754	.990	.709	.681	.913
.745	.792	.998	.694	.716	.966
.730	.826	.966	.673	.760	.999
.715	.856	.905	.654	.798	.987
.699	.883	.814	.635	.831	.940
.682	.908	.700	.616	.861	.863
.663	.931	.567	.597	.887	.764
.640	.953	.416	.576	.912	.643
.608	.973	.252	.552	.935	.508
.545	.992	.080	.522	.956	.362
0.513:	0.996	0.036	.483	.976	.208
			.442	.988	.102
			0.405	0.994	0.050

TABLE 1—*Continued*

$\delta_1=16.90$ $\tau_c^{1/4}=2.167$	$M\mu^2=56.0$ $(\zeta/\tau^{1/4})_{max}=1.778$		$\delta_1=11.51$ $\tau_c^{1/4}=3.020$	$M\mu^2=19.3$ $(\zeta/\tau^{1/4})_{max}=3.174$	
$r/R=1/x$	T/T_c	ρ/ρ_{max}	$r/R=1/x$	T/T_c	ρ/ρ_{max}
0.868	0.146	0.018	0.832	0.105	0.010
.814	.218	0.059	.806	.124	.017
.786	.260	0.097	.777	.148	.028
.755	.309	0.161	.734	.186	.055
.720	.367	0.260	.698	.222	.091
.697	.406	0.342	.676	.245	.122
.680	.436	0.412	.646	.278	.174
.666	.462	0.473	.625	.303	.219
.644	.502	0.576	.602	.331	.278
.627	.535	0.661	.575	.366	.361
.605	.574	0.762	.555	.394	.431
.582	.617	0.859	.535	.420	.502
.562	.653	0.926	.515	.450	.582
.545	.683	0.968	.494	.480	.664
.529	.710	0.992	.468	.518	.766
.514	.734	1.000	.443	.557	.856
.500	.756	0.994	.403	.616	.958
.487	.776	0.979	.372	.662	.997
.474	.795	0.953	.346	.700	.996
.449	.829	0.880	.313	.748	.948
.424	.859	0.785	.280	.793	.857
.399	.886	0.675	.248	.833	.739
.373	.911	0.553	.216	.872	.597
.344	.934	0.426	.177	.914	.418
.312	.956	0.296	.131	.958	.211
.271	.976	0.164	.104	.978	.112
.244	.986	0.100	.082	.990	.049
.200	.995	0.035	.069	.995	.024
0.120	0.9995	0.004	0.051	0.999	0.005

pressed as a fraction of the central temperature T_c, and the third column gives the density in units of the maximum density occurring in the given model. These relative units are used because of the homology invariance of the models considered. However, the scale factor can be determined for any assigned value of R, and by multiplying the quantities in columns 2 and 3 by the appropriate factors the physical variables can be expressed in any desired units. For this purpose the values of $\tau_c^{1/4} \sim T_c$ and $(\zeta/\tau^{1/4})_{max} \sim \rho_{max}$ are given at the top of the table for each solution.

The density and pressure distributions for six of the models are presented graphically in Figure 1.

We are now able to determine the slope of the mass-luminosity

relation. To put it in the usual form, the equations given above for M and L are written

$$\log M = \log 1.117 \odot - 2 \log \mu + \log \delta_2^{1/2}(\delta_1 + \delta_2)$$

$$2.5 \log L = 2.5 \log \frac{1.471 \times 10^4}{\mu^2 \kappa} - 2.5 \log \delta_2^{3/2} .$$

When $\log M\mu^2$ is plotted against $2.5 \log \delta_2^{3/2}$, as in Figure 2, we obtain the ordinary mass-luminosity diagram except that the curve

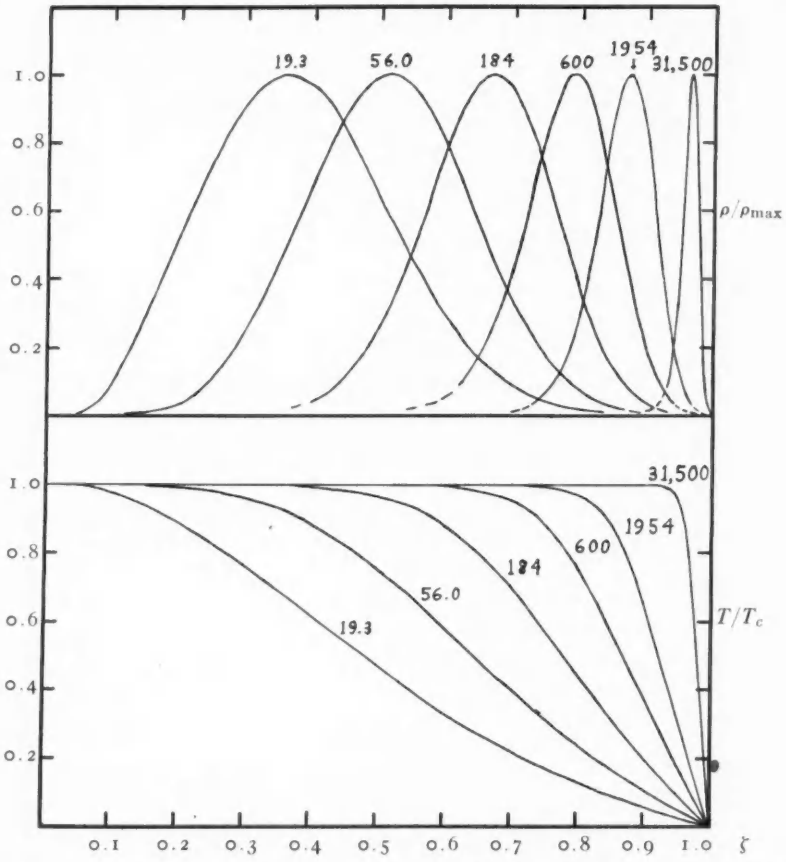

FIG. 1.—Distribution as density and temperature in the point-source models. Abscissae are given as fractions of the total radius.

is displaced both horizontally and vertically by constants depending upon the values assigned to μ and κ. For large masses the slope of the curve is much less than for small masses, where the point-

source model is known to agree with the Standard Model in predicting $L \sim M^{4.5}$, approximately.

The computed values are collected in Table 2, in which the last column represents the quantity ξ^* defined by Chandrasekhar[10] as that fraction of the radius which incloses 90 per cent of the total mass. It is thus a measure of the degree of central condensation of the matter of the star, and is about 0.43 for main-sequence stars.

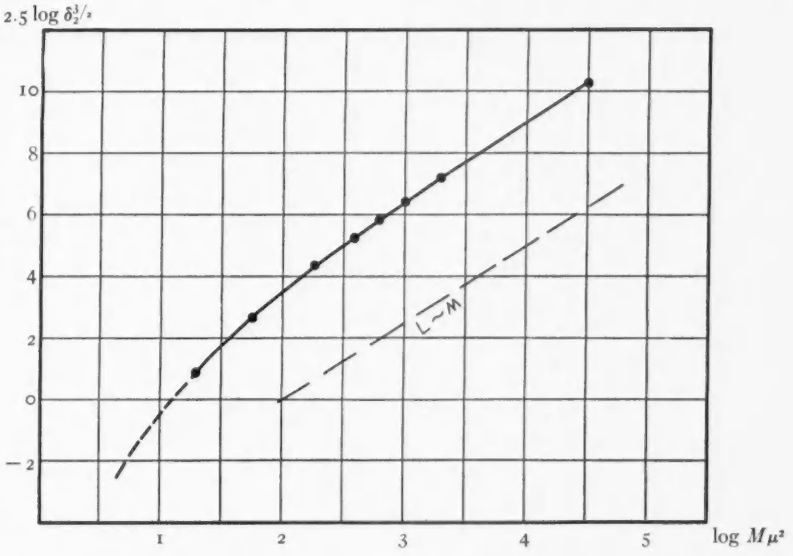

FIG. 2.—Mass-luminosity diagram for point-source models. Ordinates are proportional to absolute magnitudes. The broken line below the main curve represents the slope corresponding to $L \sim M$.

For our model ξ^* can be found by substituting dz/dt for δ_1 in the mass equation, which then runs

$$M_\xi = 1.117 \odot \mu^{-2}\delta_2^{1/2}\left(\frac{dz}{dt} + \delta_2\right).$$

Dividing by the expression for M and setting

$$\frac{M_\xi}{M} = 0.9 \qquad \text{for} \qquad \xi = \xi^*,$$

we find

$$\left(\frac{dz}{dt}\right)_{\xi^*} = 0.9\,(\delta_1 + \delta_2) - \delta_2.$$

[10] *Op. cit.*, chap. viii, p. 292.

This expression gives $(dz/dt)_{\xi^*}$ and hence $(d\zeta/d\tau)_{\xi^*}$, so that ξ^* can be obtained by interpolation from the numerical solution for the given model.

For actual stars ξ^* can be found when M, L, R, and μ are known, and, since the massive Trumpler stars are known to have a relatively low degree of central condensation, it is of interest to note that the values determined for them by Chandrasekhar[11] have the same general run as those computed for point-source models of the same order of mass. This agreement is merely suggestive, for, as Chandrasekhar

TABLE 2

δ_1	δ_2	$M\mu^2$	$L\mu^2\kappa\times10^{-4}$	log $M\mu^2$	log $\delta_2^{3/2}$	ξ^*
11.51	1.71	19.3	0.328	1.29	0.348	0.652
16.9	5.15	56.0	1.72	1.75	1.068	.725
29.0	14.4	184	8.00	2.26	1.74	.805
42.6	25.4	383	18.85	2.58	2.11	.852
54.3	35.6	600	31.2	2.78	2.33	.873
73.1	52.7	1,020	56.3	3.00	2.58	.897
107.3	84.9	1,954	111	3.29	2.88	.922
625	566	31,500	1,970	4.50	4.13	0.979

has pointed out,[12] any model characterized by sufficiently extensive negative density gradients will give large values for ξ^*. On the other hand, it may be further noted that, if the mass-luminosity relation for the point-source model is fitted to the observational curve for ordinary stars by extrapolating it to small masses, it represents very well the position of the Trumpler stars in the diagram.[13]

In considering the possible physical significance of this model, it must be emphasized again that the properties derived represent an extreme limiting case in the discussion of the mass-luminosity relation.

These computations were undertaken at the suggestion of Professor Chandrasekhar, and it is a pleasure to acknowledge helpful discussions with him at all stages of the work.

YERKES OBSERVATORY
January 1939

[11] *Ibid.*, p. 314. [12] *M.N.*, **97**, 149, 1936.

[13] For the observed mass-luminosity relation see Kuiper, *Ap. J.*, **88**, 489, 1938.

ON THE COLOR OF P CYGNI

FRANCES SHERMAN AND W. W. MORGAN

ABSTRACT

From a comparison of color excesses of stars near P Cygni and located at about the same distance from the sun, it is found that the color excess of P Cygni is partly due to interstellar reddening and partly to conditions in the immediate neighborhood of the star itself.

Attention is called to a systematic progression of determinations of color excesses apparently depending on the range of wave lengths observed.

I. INTRODUCTION

At the present time the evidence seems conclusive that most, if not all, of the reddening observed in distant ordinary B stars is interstellar in origin. In the case of the B and A supergiants there may be intrinsic differences of a minor amount from dwarfs of the same spectral type, but the greater part of the reddening found for these objects also seems definitely interstellar in nature.

The B stars having strong emission lines, however, seem to behave differently. They were found by E. G. Williams[1] to be systematically too red for their distances as determined from the interstellar K line in their spectra. He suggested, as the probable explanation, that their light is subjected to selective scattering in an extensive atmosphere surrounding the star; the existence of such extensive atmospheres had been predicted earlier by Struve from his theory of the origin of bright lines.

Further evidence on the subject has been found recently from observations of γ Cassiopeiae. Chalonge and Safir,[2] and Greaves and Martin,[3] found that the color temperature of this Be star decreased considerably during its recent light and spectral variations. From gradients determined by the Greenwich observers the temperature was found to be 16,100° in 1926 and 9,200° in the latter part of 1937. The first temperature corresponds to that of a star of type B8, while the latter is similar to one of type A5–F0 as determined at Greenwich. In the case of the changes in γ Cassiopeiae there can be little doubt that they were due to conditions in the immediate

[1] *Ap. J.*, **79**, 303, 1934. [2] *C.R.*, **203**, 1329, 1936. [3] *M.N.*, **98**, 434, 1938.

neighborhood of the star; we thus have an individual case in which selective absorption has been shown to exist as an atmospheric phenomenon in a Be star.

It is the purpose of the present paper to attempt to find what part of the color excess of P Cygni is due to ordinary selective absorption and what part—if any—is peculiar to the neighborhood of the star itself. This was done by determining the color excesses of stars near P Cygni in the sky and situated at the same distance from the sun.

II. THE DISTANCE OF P CYGNI

Spectroscopic determinations of the luminosity of P Cygni are of doubtful value, since most of the observed absorption features do not originate in the star itself but in the expanding envelope. The safest procedure is probably to use the intensities of the interstellar K and D lines as criteria of distance. For the D lines the intensities and reduction curve by Merrill[4] were used, and an apparent distance modulus of 9.1 was found. This was determined from a general distance-intensity relation for all stars, as regional differences had been found by Merrill to be fairly small.

A different procedure was followed in the case of the K line. The measured total absorptions determined by Williams[5] (unreduced to an exponential contour[6]) were plotted against apparent distance moduli for stars for which Williams had determined spectroscopic absolute magnitudes.[7] Stars from galactic longitude 340° to 85° were included which are within 10° of the galactic equator and which have spectral types between Bo and B5. The Be stars were omitted. From the K line an apparent distance modulus of 9.5 was found.

III. THE COMPARISON STARS

Fifteen stars located within about half of a degree of P Cygni were selected to serve as comparisons. For nine of these having spectral types between B8 and A5 the Draper types were used, and the assumption was made that they are main-sequence stars. Each star

[4] *Ap. J.*, **86**, 297, 1937; **87**, 120, 1938. [5] *Ibid.*, **79**, 291, 1934.

[6] Irregularities in the observed contours of interstellar K and D lines, as found by Beals, make the use of the uncorrected total absorption preferable.

[7] *Ap. J.*, **83**, 333, 1936.

was assumed to have the absolute magnitude of the mean of the main-sequence stars of its type, as estimated from stars in the neighborhood of the sun. Spectra of the other objects were obtained at the Yerkes Observatory with low-dispersion cameras attached to the Bruce spectrograph.

The luminosities of the B stars were based principally on the intensities of the hydrogen lines, while the luminosity of the F5 dwarf was determined from the enhanced lines commonly used for stars of this type. The luminosity standards for the early-type stars were γ Orionis (B2) and χ^2 Orionis (cB1); the calibration of giants, intermediates, and dwarfs by Williams was used. The absolute magnitude of γ Orionis was found to be -3.6 by Kapteyn[8] in his study of the parallaxes of the stars in the "Orion Group," and it was considered to be typical of luminosity class iB2. The apparent distance moduli of the comparison stars range from 5.5 to 13.3. As the mean of the two determinations of the modulus of P Cygni is 9.3, the selection of comparison stars can be considered satisfactory for investigating the amount of selective absorption.

IV. THE COLOR INDICES

For the determination of the color indices of the comparison stars and of P Cygni, the method of effective wave lengths was used. A coarse wire grating having approximately equal bars and spaces was used in connection with the 24-inch reflector, which was diaphragmed to 15 inches to improve the photometric field. Eastman Ortho Press plates were used. The exposures were made at the same altitude as the pole, and the transformation to color indices was made by means of direct comparisons with the international color indices of the North Polar Sequence. The exposure times were, in general, the same on the field of P Cygni and on the pole; they ranged in duration from a few seconds to twenty minutes. The question of possible systematic errors depending on the variation of exposure time was investigated, and it was found that any such errors were so small that they were within the mean error of one observation.

The combination of aluminized reflector and orthochromatic emul-

[8] *Ibid.*, **47**, 463, 1918.

sion was found to be very sensitive to slight changes in color index, so that the internal accuracy of the color indices is good. A tabulation of effective wave lengths and measured distances between the maxima of the first-order spectra is given in Table 1, where the

TABLE 1

Star	Sp.	C_I	$2D$	λ_{eff}
NPS 2	Ao	−0.08	402	0.433
3	Fo	+0.18	414	.446
3s	F2	+0.31	420	.452
1r	Ma	+1.59	468	0.504

columns give: (1) the star's designation in the North Polar Sequence; (2) the Henry Draper spectral type; (3) the color index on the International System; (4) the measured distances between the maxima of the first-order spectra in μ; and (5) the effective wave length, also expressed in μ. There is a change in distance of 66 μ between Ao and Ma; the uncertainty of measurement is about ± 2 μ. Some of the comparison stars were observed only once, while the color index of others depends on from two to five observations.

V. THE INTRINSIC COLORS

As the North Polar Sequence does not contain stars of early B spectral types, the system of normal color indices for such stars is rather uncertain. The procedure adopted was to adapt the intrinsic colors derived in an earlier paper.[9] These colors were on the system of Bottlinger's photoelectric measures. They were first transformed to King's system (King's photographic magnitude minus the visual magnitude in the *Revised Harvard Photometry*) from a plot of stars common to both observers. A scale and zero-point correction was then applied to reduce the system as nearly as possible to the North Polar Sequence. This was done by making the interval Ao–gKo, 1.12 mag. and assigning bright Ao stars a color index of zero. The system of intrinsic color indices so derived is given in Table 2. As the bright stars of the Polar Sequence are reddened by about a tenth of a magnitude, this correction was applied to the colors derived for the comparison stars to determine the amount of interstellar reddening.

[9] *Ibid.*, **87**, 471, 1938.

VI. THE OBSERVED COLOR EXCESSES

The resulting color indices and color excesses for the fifteen comparison stars and for P Cygni are given in Table 3. The columns

TABLE 2

Type	C	Type	C
Bo	−0.58	dF5	+0.37
B2	−0.45	dF8	0.48
B5	−0.30	dGo	0.55
B8	−0.23	dG5	0.69
Ao	0	dKo	0.90
A2	+0.13	dK5	1.22
A5	+0.21	dK6	1.47
Fo	+0.23		
gF5	+0.42	cF5	0.44
gF8	+0.58	cF8	0.75
gGo	+0.74	cGo	1.11
gG5	+0.92	cG5	1.30
gKo	+1.12	cKo	1.58
gK2	+1.26	cK2	1.77
gK5	+1.67	cK3	1.99
gMo	+1.88	cMo	+2.15

TABLE 3

HD	m_{vis}	Sp.	M	$m-M$	C_1	ΔC
193184	8.5	dF5	+3.0	5.5	0.23	−0.04
193612	9.2	A2	+1.5	7.7	.15	+ .12
228944	9.8	A3	+1.5	8.3	.18	+ .12
228623	10.1	A3	+1.5	8.6	.26	+ .20
228793	10.1	dA2	+1.5	8.6	.20	+ .17
193537	9.2	Ao	+0.5	8.7	.18	+ .28
228618	10.7	A5	+2.0	8.7	.24	+ .13
228598	9.8	Ao	+0.5	9.3	.22	+ .32
228906	10.1	Ao	+0.5	9.6	.17	+ .27
228932	10.1	B8	−0.5	10.6	.15	+ .48
228807	8.3	iB2	−3.1	11.4	.16	+ .71
193516	8.8	iB2	−3.1	11.9	.21	+ .76
193443	7.7	i+B1	−4.7	12.4	.15	+ .77
193183	7.1	gB1	−5.5	12.6	.18	+ .80
193444	9.0	i+B2	−4.3	13.3	.22	+ .77
P Cygni	4.9	B1p	.....	9.1 (D) 9.5 (K)	0.22	+0.86

give: (1) the Henry Draper number; (2) the visual magnitude; (3) the spectral type (if there is no prefix the type is that of the *Henry*

Draper Catalogue; the other stars were reobserved at Yerkes and were assigned to luminosity classes; the prefix "i" corresponds to stars of intermediate luminosity, similar to γ Orionis; the classification "i+" is assigned to stars intermediate in luminosity between γ Orionis and the supergiant χ^2 Orionis); (4) the absolute magnitude; (5) the apparent distance modulus; (6) the color index on the International System; and (7) the color excess, found by comparing (6)

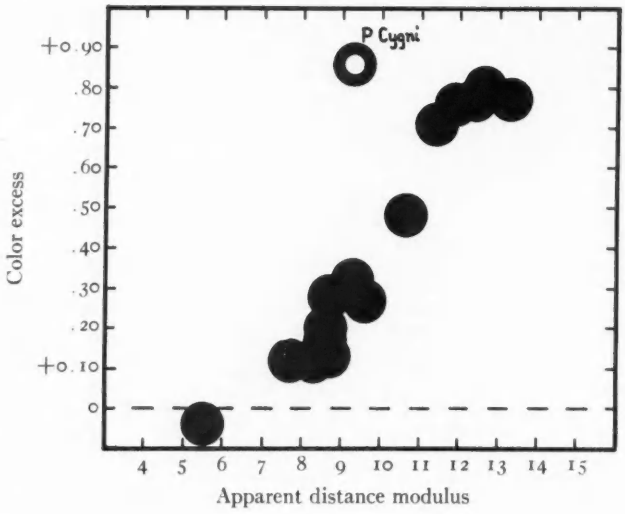

FIG. 1

with Table 2 and adding 0.1 mag. to correct for the selective absorption in the Polar Sequence.

The apparent distance moduli and color excesses are plotted in Figure 1. The star P Cygni seems considerably redder than it should be if the reddening is due to interstellar selective absorption exclusively. If Figure 1 is taken at its face value, we find that interstellar absorption accounts for a reddening of about three-tenths of a magnitude, while the residual color excess of about half a magnitude must originate in the vicinity of the star itself.

VII. CONCLUSIONS

There are, however, several factors which must be considered before we accept the quantitative data of Figure 1. They are: (*a*) the

spectral type of P Cygni; (*b*) the system on which the color excesses are expressed; (*c*) the possibilities of systematic errors in the spectroscopic luminosities on which the apparent distance moduli are based.

a) *The spectral type of P Cygni.*—This is a factor which may be of considerable importance. The spectral type is based on the ordinary strong absorption lines; these lines, however, do not originate in the star itself but in an expanding shell where conditions of excitation may be very different from those in a normal stellar reversing layer. If the continuous radiation originates in the star itself—which seems to be the case—our intrinsic color as determined from the spectral type may be considerably in error. We may make the problem a little more definite by stating that if the continuous radiation near the star has a spectral distribution similar to a star of spectral type Ao, then there is no reddening which could not be explained by interstellar selective absorption. That this could be the case is, of course, quite unlikely, and it seems highly probable that at least part of the color excess is due to material near the star.

b) *The system on which the color excesses are expressed.*—A different kind of difficulty, but one which complicates the comparison of various determinations of color excesses, is a marked dependence of the amount of the color excess on the spectral range observed. The values by various observers for five stars are given in Table 4. The color indices as observed are listed, and the colors are referred to those of stars of the main sequence by means of the comparison stars used by each observer. The last horizontal line gives an indication of the "base line" used by showing the interval Ao–gKo. The largest interval is that of the spectrophotometric measures, and we find that the resulting color excesses are considerably larger than those determined by Stebbins and Huffer with the photoelectric cell. On the other hand, there seems to be a systematic effect among the photoelectric observers themselves which is also dependent on the base line used. The stars 55 Cygni and χ^2 Orionis, which are common to all observers, show a general decrease in color excess as the base line is decreased. The star σ Cygni is especially striking; from the measures of Becker and Bottlinger it would be considered to be unaffected by selective absorption, while the spectrophotometric results suggest the opposite conclusion. It is possible that this disa-

greement may be due to the same factors which cause the disagreement between the photographic and photoelectric data of the North Polar Sequence.

c) *The spectroscopic luminosities.*—As the most distant stars in Table 3 are also the most luminous, any systematic error in the absolute magnitudes of these objects will alter the slope of the distance-reddening diagram. It is unfortunate that fainter stars of lower luminosity could not be added to the comparison stars to check the

TABLE 4

COLORS OF REDDENED STARS REFERRED TO MAIN SEQUENCE INTRINSIC COLORS

Star		Spectrophotometric*		Stebbins (p.-e.) Huffer		Becker (p.-e.)		Bottlinger (p.-e.)	
		T	C_{sp}	C	C_{sp}	C	C_{sp}	C	C_{sp}
P Cygni	B1p	5700°	g3	+0.06	a9	−0.08	a2	.....	.....
55 Cygni	cB2	5500	g5	+. 05	a8	− .06	a3	−0.54	a2
χ^2 Orionis	cB2	6100	f9	−0.02	a3	− .07	a3	.58	a0
σ Cygni	cA0	7700	f0	.....	.....	− .15	b9	.60	b9
ν Cephei	cA2	5700	g0	.....	.....	+0.01	f0	−0.47	f2
A0–gK0.....		(1.1)		0.74		0.59		0.53	

* Miss Payne's reduction (*The Stars of High Luminosity*, p. 102) of the results of Hertzsprung, Gerasimovič, and the Greenwich observers.

luminosities of the latter. New spectrographic equipment is now available which will allow the extension to fainter stars, and we hope to strengthen the evidence of the diagram for the more distant stars next season. It seems safe to say at the present time, however, that a change in slope sufficient to make P Cygni lie on the curve seems exceedingly unlikely.

With due regard to the complications mentioned, we may conclude that the color excess of P Cygni is considerably greater than that of other stars in its neighborhood at the same distance from the sun, and that a considerable part of the observed reddening is probably due to physical conditions in the immediate vicinity of the star.

YERKES OBSERVATORY
WILLIAMS BAY, WISCONSIN
January 3, 1939

OBSERVATIONS MADE WITH THE NEBULAR SPECTROGRAPH OF THE McDONALD OBSERVATORY. II*

OTTO STRUVE AND C. T. ELVEY

ABSTRACT

A series of spectrograms in Monoceros and Canis Major reveal a number of new emission nebulosities, some of which seem to be unrelated to any individual stars while others form distinct groups which are related to O or B stars. A spectrophotometric study of $H\alpha$ and $H\beta$ in the outer loop of Orion near BD+1°1126 gives $n_4 = 4$ cm^{-2} and $n_3 = 3$ cm^{-2}. It is estimated that the faintest recorded emission nebulosities have three times fewer atoms in the fourth and the third energy-levels of H, per square centimeter. This agrees satisfactorily with former estimates.

The present series of observations is a continuation of those published in former issues of this *Journal*.[1] The instrument and the technique were the same as those used before, but the Agfa Superpan Press film was hypersensitized with ammonia, in accordance with the method of Bowen and Wyse.[2] A marked increase in speed was obtained. The numbering of the regions follows chronologically that of our previous series.

The emission features of the spectrum of the night sky were relatively faint throughout the present series of observations. This was especially valuable in distinguishing the nebular emission line [*O* II] 3727, which was of even greater use in this series than $H\alpha$. We are not prepared to state that there is a real systematic difference in the ratio [*O* II]/$H\alpha$ between the summer Milky Way (Cygnus, Cepheus) and the winter Milky Way (Monoceros, Canis Major). But there can be no doubt that the large diffuse nebula around S Monoceratis is especially strong in [*O* II]. This, incidentally, explains our former observation that this nebula is relatively weak when photographed in red light.[3]

The preponderance of emission spectra in Table 1 is partly due to the fact that we have included in our program a number of known

* *Contributions from the McDonald Observatory, University of Texas*, No. 9.

[1] *Ap. J.*, **89**, 119, 1939.

[2] *Pub. A.S.P.*, **50**, 305, 1938.

[3] Struve, *Ap. J.*, **86**, 98, n. 13, 1937.

diffuse nebulosities for which hitherto no spectra were available. The great majority of these extended films of nebulosity in and near the Milky Way have emission spectra. However, several regions show no trace of nebulosity on the direct photographs, although the spectrograph reveals conclusive evidence of emission by interstellar gaseous matter. Only one of the regions listed in the table was located far from the Milky Way. It showed no emission. In addition, the evidence of the comparison spectra is instructive: they were usually taken 30°–40° north of the Milky Way region. This would place them about 10° north of the eastern edge of the Milky Way. Not one of these exposures reveals a trace of emission.

The principal purpose of the observations was to obtain a determination of the number of hydrogen atoms per square centimeter of a standard nebula. The value used in our former work ($n_3 = 10$ atoms/cm^2)[4] depended upon a comparison with the Orion nebula for which Ambarzumian[5] had determined the numbers of hydrogen atoms in the fourth, fifth, and sixth energy-levels. An independent determination is greatly needed because of the astrophysical significance of these quantities.[6]

We have chosen for this purpose the outer loop of Orion, near the star BD+1°1126. The nebula is relatively strong at this point and is fairly uniform over the length of our slit. We estimate that the faintest emission nebulae recorded by us are about three times fainter than the region selected as standard. The spectral type of the standard star is G5, and the photographic magnitude is 6.95, according to the *Henry Draper Catalogue*. Dr. C. K. Seyfert has very kindly determined the magnitude with the 6-inch UV refractor. His results are

$$\text{BD} + 1°1126 \begin{cases} \text{photographic magnitude } 6.67 \\ \text{photovisual magnitude } 5.92 \end{cases}$$

Dr. W. W. Morgan has redetermined the spectral type at the Yerkes Observatory and has found it to be G5 on his system. The lumi-

[4] *Ibid.*, **88**, 367, 1938.

[5] *Zs. f. Ap.*, **6**, 112, 1933.

[6] See Struve, *Proc. Nat. Acad. Sci.*, **25**, 36, 1939; Struve, Wurm, and Henyey, *ibid.*, p. 67; Struve, *Zs. f. Ap.*, **17**, 316, 1939.

nosity classification by Morgan makes it a subgiant or a dwarf, and the color index on the international system should therefore be +0.7 mag—in close agreement with the determination by Seyfert.

The procedure was quite similar to that adopted by Ambarzumian. The star served as guiding star for the nebula. Hence, there are no corrections for extinction. The exposure was obtained on January 18/19 (see Region No. 41), and the star was trailed uniformly over a distance of 11′ along the slit. Sensitometer exposures were used to construct the characteristic curves separately for each wave length. The width of the slit corresponded to 2′.4.

The only important difference between our work and that of Ambarzumian consisted in the fact that in our instrument the slit acts as a diaphragm which reduces the intensity of the star but leaves the nebula unaffected. For the equivalent slit width of 50 mm the correction resulting from this effect corresponds to somewhat less than a factor of 2. We shall adopt a factor of 2 in order to compensate for small losses of starlight at the ends of the trailed image and because of optical imperfections in the plane mirrors.

Although the spectral type is not exactly that of the sun, the resulting error is insignificant if we use the photographic magnitudes of star and sun for $H\beta$, etc., and the photovisual magnitudes for $H\alpha$.

We apply Ambarzumian's expression, corrected for the diaphragming effect of the slit:

$$\log \frac{E_{n\lambda}}{E_{\odot\lambda}} = \log P_\lambda - 0.4(m_* - m_\odot) + \log S - \log 2 ,$$

where $E_{n\lambda}$ is the energy radiated by 1 cm² of the nebula per second in unit solid angle, in the monochromatic line λ, $E_{\odot\lambda}$ the energy radiated by 1 cm² of the sun's surface per second per angstrom unit in unit solid angle, near wave length λ, P_λ the ratio of intensity in the monochromatic nebular image, per square minute of arc, to intensity in the star spectrum at neighboring wave lengths, per angstrom unit, over the full width of the spectrum, expressed in minutes of arc, and S the surface of the sun in square minutes of arc. Since the linear dispersion on our plates is approximately 1000

A/mm at $H\alpha$ and 440 A/mm at $H\beta$, we can easily derive P_λ for both lines and then compute $\log E_{n\lambda}/E_{\odot\lambda}$. The results are:

$$H\beta\text{: } \log \frac{E_{n\lambda}}{E_{\odot\lambda}} = -10.26\,,$$

$$H\alpha\text{: } \log \frac{E_{n\lambda}}{E_{\odot\lambda}} = -9.56\,.$$

For $H\beta$ in the Orion nebula, Ambarzumian found $\log E_{n\lambda}/E_{\odot\lambda} = -7.95$. Hence, our nebula is about 2000 times fainter. Remembering that we have estimated our faintest nebulae to be about three times fainter than the standard in the outer loop of Orion, we conclude that our former ratio of 1000 was too small by a factor of 6. Hence, the number of atoms in the fourth energy-level of H for the outer loop of Orion is

$$n_4 = 4 \text{ cm}^{-2}\,,$$

and for the faintest recorded nebulae

$$n_4 = 1 \text{ cm}^{-2}\,.$$

For $H\alpha$, which was not observed by Ambarzumian, we first compute the value of $E_{n\lambda}$ and then derive the number of atoms in the third energy-level:

$$n_3 = \frac{4\pi E_{n\lambda}}{h\nu A_{31}}\,,$$

where $A_{31} = 0.43 \times 10^8 \text{ sec}^{-1}$. The result is, for the outer loop of Orion,

$$n_3 = 3 \text{ cm}^{-2}\,,$$

and for the faintest recorded nebulae,

$$n_3 = 1 \text{ cm}^{-2}\,.$$

This result agrees reasonably with the one used in our previous computations ($n_3 = 10 \text{ cm}^{-2}$), but the precision of the measurement

is, of course, very low. It is, therefore, not disturbing that n_3 is slightly smaller than n_4. Both results may easily be in error by a factor of as much as 10.

No. 36.—Guiding star 15 S Mon. 1939, Jan. 14/15. Exp. 3^h45^m. Comparison mirror $\Delta\delta = +30°$. Slit eq. 40 mm. [*O* II] 3727 is very conspicuous; *Hα* is strong; *Hβ*, *Hγ*, *Hδ*, and N_1 are present. The emission is slightly stronger west of the star than at the eastern end of the slit. This nebula has already been observed by Greenstein and Henyey.[7] The most conspicuous feature is the great strength of [*O* II] 3727 and the relative weakness of *Hα*. The spectral type of the guiding star is O7s.

No. 37.—Guiding star BD+9° 1376. 1939, Jan. 14/15. Exp. 4^h. Comparison mirror $\Delta\delta = +30°$. Slit eq. 40 mm. This region is about 1° east of No. 36, and the spectrum is closely similar. [*O* II] 3727 is very strong; *Hα* is relatively weak; N_1 is very weak; *Hβ* and *Hγ* are faint. The Balmer decrement seems to be low.[7] The emission weakens toward the east but is still fairly conspicuous at the eastern end of the slit (45′ west of the guiding star). This agrees with the extent of the large nebulosity photographed by Ross.[8]

No. 38.—Guiding star BD+10°1335. 1939, Jan. 15/16. Exp. 4^h4^m. Comparison mirror $\Delta\delta = +30°$. Slit eq. 40 mm. This region is about 4° east of No. 36. There is no definite emission, but we suspect an exceedingly faint trace of [*O* II] 3727. This may, however, be the night-sky line of the same wave length.

No. 39.—Guiding star BD+10°1335. 1939, Jan. 15/16. Exp. 4^h7^m. Comparison mirror $\Delta\delta = +30°$. Slit eq. 40 mm. This region is about 1° west of No. 36. The small bright nebulosity, NGC 2245, which surrounds the guiding star shows no trace of emission, and its spectrum must be purely continuous. This agrees with the observation by Hubble.[9] There is, however, superposed a weak emission spectrum, strong at the eastern end of the slit and weak at the western end, which evidently represents an extension of the large nebula around S Mon. [*O* II] 3727 is fairly strong, while *Hα* is very weak. The spectral type of the guiding star is B8, according to the *Henry Draper Catalogue*.

[7] *Ap. J.*, **87**, 80, 1938.

[8] *Ibid.*, **67**, Pl. VI, 1928.

[9] *Ibid.*, **44**, 196, 1916; **56**, 173, 405, 1922.

TABLE 1

OBSERVATIONS MADE WITH THE NEBULAR SPECTROGRAPH

No.	Object	Guiding Star	Date	Identification*	Result
36....	Nebula NGC 2264	15 S Mon	1939, Jan. 14/15	Ross 35; 168 mm from right; 162 mm from bottom	Strong emission
37....	Nebula	BD+ 9°1376	Jan. 14/15	Ross 35; 148 mm from left; 160 mm from bottom	Strong emission
38....	Milky Way	BD+10°1335	Jan. 15/16	Ross 35; 107 mm from left; 165 mm from bottom	Probably no emission
39....	NGC 2245	BD+10°1159	Jan. 15/16	Ross 35; 126 mm from right; 162 mm from bottom	Emission
40....	IC 448	BD+ 7°1337	Jan. 16/17	Ross 35; 139 mm from right; 122 mm from bottom	Emission
41....	Outer loop of Orion	BD+ 1°1126	Jan. 17/18	Ross 34; 114 mm from left; 128 mm from top	Emission
42....	Milky Way	BD+ 8°1438	Jan. 17/18	Ross 35; 167 mm from right; 135 mm from bottom	Strong emission
43....	Milky Way	BD+15°1075	Jan. 19/20	Ross 35; 44 mm from right; 79 mm from top	Strong emission
44....	Milky Way	30 τ CMa	Jan. 19/20	Ross 38; 112 mm from left; 146 mm from bottom	Emission
45....	Nebula IC 2177	BD−10°1862	Jan. 20/21	Ross 37; 82 mm from right; 164 mm from top	Strong emission
46....	Milky Way	BD−10°1892	Jan. 22/23	Ross 37; 95 mm from right; 159 mm from top	Emission
47....	.....	ρ Leonis	Jan. 22/23	.....	No emission
48....	Milky Way	BD− 8°1862	Jan. 23/24	Ross 37; 139 mm from right; 134 mm from top	Emission

* The co-ordinates are only approximate. Differences of the order of 1 mm in each co-ordinate are possible on different prints of the same photograph of Ross's *Atlas of the Milky Way*.

No. 40.—Guiding star BD+7°1337. 1939, Jan. 16/17. Exp. 5^h. Comparison mirror $\Delta\delta = +30°$. Slit eq. 40 mm. This region is about 3° southwest of No. 36. [*O* II] 3727 is a very strong emission line, but *Hα* is rather weak. The oxygen line is of uniform brightness along the entire slit and must belong to the large nebula around S Mon. Since there is no strengthening of the emission lines near the guiding star, we believe that the faint nebula, IC 448, surrounding it has a continuous spectrum. The spectrum of the guiding star is Aop and the lines are described in the *Henry Draper Catalogue* as very narrow and sharply defined, resembling in intensity those of *η* Leonis.

No. 41.—Guiding star BD+1°1126. 1939, Jan. 17/18. Exp. 4^h5^m. Comparison mirror $\Delta\delta = +40°$. Slit eq. 40 mm. 1939, Jan. 18/19. Exp. 4^h. Slit eq. 50 mm. *Hα* is very strong; [*O* II] 3727 is somewhat fainter, confirming the reality of the unusual strength of the oxygen line (or weakness of *Hα*) in the large nebula around S Mon. *Hβ* and *Hγ* are faint; N_1 is not visible on our plate. This observation confirms in every detail that by Greenstein and Henyey[10] which was made slightly farther south.

No. 42.—Guiding star BD+8°1438. 1939, Jan. 17/18. Exp. 4^h5^m. Comparison mirror $\Delta\delta = +30°$. Slit eq. 40 mm. [*O* II] 3727 is exceptionally strong; *Hα* is fairly strong; *Hβ* and *Hγ* are weak. The lines are fairly uniform along the slit. This is an extension of the nebula around S Mon.

No. 43.—Guiding star BD+15°1075. 1939, Jan. 19/20. Exp. 3^h30^m. Comparison mirror $\Delta\delta = +30°$. Slit eq. 40 mm. This region was chosen because of the strong emission nebulosity revealed in red light, by H. A. Lower.[11] This fairly large, round nebula seems not to have been recognized previously, but a careful inspection of Ross's plates No. 35 and 33 shows an exceedingly faint trace of it. Barnard's photograph[12] does not show it. The nebula must be very faint in blue and violet light. This is substantiated by our spectrum: *Hα* is very strong in emission; [*O* II] 3727 is relatively weak; *Hβ* and *Hγ* are very faint; there is no trace of N_1. The emission lines are strongly concentrated toward the middle of the slit, suggesting that

[10] *Ibid.*, **87**, 79, 1938.

[11] *Ibid.*, **89**, Pl. XIV, 1939.

[12] *Pub. Lick Obs.*, **11**, Pl. 25, 1913.

the brightest part of the nebula has a diameter of 15′–20′. However, *Hα* extends to both ends of the slit. The nebula is considerably larger than should be expected from Hubble's relation. The spectrum of the guiding star is not known. The nebula may be associated with the slightly brighter star, BD+15°1079=HD 41997, the spectrum of which is given as B in the *Henry Draper Catalogue*. The absorption lines are described as showing slight contrast to other portions of the spectrum. The photographic magnitude is 8.3. This interesting nebula deserves further study.

No. 44.—Guiding star 30 τ Can. Maj. 1939, Jan. 19/20. Exp. 3^h52^m. Comparison mirror $\Delta\delta = +50°$. Slit eq. 40 mm. This region contains no known nebulosity, but a slight milkiness on Ross's photograph suggests the possible existence of a very large diffuse nebulosity which merges into a large obscured region on the east. *Hα* is strong in emission and so is [*O* II] 3727; *Hβ* and *Hγ* are faint; N_1 is not definitely seen but may be present. The lines are slightly stronger near the eastern end of the slit than in the immediate vicinity of the guiding star. The spectral type of τ Can. Maj. is O9, and that of the neighboring star, 29 Can. Maj., is O7e.

No. 45.—Guiding star BD−10°1862. 1939, Jan. 20/21. Exp. 3^h54^m. Comparison mirror $\Delta\delta = +40°$. Slit eq. 40 mm. *Hα* and [*O* II] 3727 are very strong and decrease slightly from the guiding star toward the eastern end of the slit; *Hβ*, *Hγ*, and *Hδ* show the same structure; N_1 is clearly visible, but its structure differs from that of the other lines; it is absent west of the guiding star, is faint immediately east of it, and increases slightly in intensity toward the eastern end of the slit, 45′ from the star. The spectrum of the guiding star is B3. The strengthening of N_1 toward the east suggests that the excitation may come from the O7s star[13] BD−10°1892 = HD 54662.

No. 46.—Guiding star BD−10°1892. 1939, Jan. 22/23. Exp. 2^h30^m. Comparison mirror $\Delta\delta = +40°$. Slit eq. 40 mm. The Ross *Atlas* shows no trace of nebulosity in this region, although it lies only about 1° east of the diffuse nebula IC 2177 (Region 45). *Hα* and [*O* II] 3727 are strong over the entire length of the slit, weakening slightly toward the east; N_1 is equal to *Hβ*, thus confirming the

[13] C. H. Payne, *The Stars of High Luminosity*, p. 64, 1930.

result obtained for Region 45. The spectrum of the guiding star is O7s.

No. 47.—Guiding star ρ Leonis. 1939, Jan. 22/23. Exp. 2^h40^m. Comparison mirror $\Delta\delta = +30°$. Slit eq. 40 mm. This Bop star has a galactic latitude of $+54°$. There is no emission.

No. 48.—Guiding star BD$-8°1862$. 1939, Jan. 23/24. Exp. 3^h5^m. Comparison mirror $\Delta\delta = +40°$. Slit eq. 40 mm. This region is about 4° northeast of No. 46 and is located in a dense region of the Milky Way, without any indication of nebulosity on the direct photograph by Ross. [*O* II] 3727 is present as a faint but well-defined emission line which decreases slightly in strength near the eastern edge. There is only a suspicion of bright *Hα*, but this plate is slightly out of focus in the red part of the spectrum. The presence of emission in this normal region of the Milky Way is perhaps even more startling than the presence of emission in the star clouds of Cygnus and Cepheus.[14]

McDonald Observatory
and
Yerkes Observatory
February 2, 1939

[14] Dr. W. H. Wright has called our attention to the fact that the strong *Hα* line coincides on spectrograms of small dispersion with the forbidden doublet of *N* II, λ 6548 and λ 6584, and there is good reason to suspect that the red images of certain nebulae are due principally to this doublet (*Pub. Lick Obs.*, **13**, 217, 1918). Since the other Balmer lines, *Hβ*, *Hγ*, etc., are also often present on our spectrograms, *Hα* is doubtless a fairly strong emission line; but it is entirely possible that a large fraction of the light comes from the nitrogen doublet. If this conclusion is correct, the number of atoms which we have derived for the third quantum level of hydrogen must be somewhat reduced. However, it will not be altered sufficiently to require a revision of the computations because we are here concerned only with a precision corresponding to a factor of 3 or 4. Dr. Wright's suggestion probably accounts for the remarkable changes in the relative intensities of *Hα* and of other Balmer lines which we had heretofore interpreted as changes in Balmer decrement. Stoy (*Lick Obs. Bull.*, **17**, 181, 1935) assigns slightly weaker intensities to the [*N* II] lines than to *Hα*, in the nebulae observed by him, but it is quite possible that the combined intensity of the two [*N* II] lines in our tenuous nebulae is of the same order as that of *Hα*.

THE PHYSICAL STATE OF INTERSTELLAR HYDROGEN

BENGT STRÖMGREN

ABSTRACT

The discovery, by Struve and Elvey, of extended areas in the Milky Way in which the Balmer lines are observed in emission suggests that hydrogen exists, in the ionized state, in large regions of space. The problem of the ionization and excitation of hydrogen is first considered in a general way. An attempt is then made to arrive at a picture of the actual physical state of interstellar hydrogen. It is found that the Balmer-line emission should be limited to certain rather sharply bounded regions in space surrounding O-type stars or clusters of O-type stars. Such regions may have diameters of about 200 parsecs, which is in general agreement with the observations. Certain aspects of the problem of the ionization of other elements and of the problem of the relative abundance of the elements in interstellar space are briefly discussed. The interstellar density of hydrogen is of the order of $N = 3$ cm^{-3}. The extent of the emission regions at right angles to the galactic plane is discussed and is found to be small.

I

The recent discovery, by Struve and Elvey,[1] of extended regions in the Milky Way showing hydrogen-line emission has opened up new and highly important possibilities for the study of the properties of interstellar matter. From the observed strength of *Hα* in the emission regions, Struve[2] has calculated the density of interstellar hydrogen. Also, he has analyzed the problem of the ionization of interstellar calcium and sodium, taking account of the presence of ionized hydrogen.

In the present paper the problem of the ionization and excitation of interstellar hydrogen is first considered in a general way. Based upon the observed intensities of interstellar hydrogen emission, an attempt is then made to arrive at a picture of the actual physical state of interstellar hydrogen. Finally, certain aspects of the problem of the ionization of other elements and of the problem of the relative abundance of the elements in interstellar space are briefly discussed.

II

Eddington[3] has considered the problem of the ionization of interstellar hydrogen and has expressed the opinion that, in a normal re-

[1] *Ap. J.*, **88**, 364, 1938; **89**, 119, 1939. [2] *Proc. Nat. Acad. Sci.*, **25**, 36, 1939.

[3] *M.N.*, **95**, 2, 1934; *Observatory*, **60**, 99, 1937.

gion of interstellar space, hydrogen is entirely un-ionized, the reason being that the ionizing ultraviolet radiation is strongly absorbed by the interstellar hydrogen. The result of the analysis given below tends to confirm Eddington's view with the modification, however, that high-temperature stars, and especially clusters of such stars, are capable of ionizing interstellar hydrogen in regions large enough to be of importance in problems of interstellar space.

In the immediate neighborhood of a star, interstellar hydrogen will be ionized. With increasing distance from the star the proportion of neutral hydrogen atoms increases, and hence the absorption of the ionizing radiation increases. Ultimately, the ionizing radiation is so much reduced that the interstellar hydrogen is un-ionized. Our problem is to derive an expression for the extent of the ionized region as a function of the temperature and absolute magnitude of the star and the density of interstellar hydrogen. A somewhat similar problem has been considered by the author in another connection.[4]

Consider a point in interstellar space at the distance s from a star of temperature T and radius R. Let the number of neutral hydrogen atoms per unit volume be N'; the number of hydrogen ions, N''; and that of free electrons, N_e. The degree of ionization at s is determined[4] by the equation

$$\frac{N''N_e}{N'} = \frac{(2\pi m_e)^{3/2}}{h^3}\,\frac{2q''}{q'}\,(kT)^{3/2}e^{-I/kT}\cdot\sqrt{\frac{T_{el}}{T}}\cdot w\,e^{-\tau_u}. \qquad (1)$$

Here I is the ionization potential; q'' and q' are the statistical weights of the ion and the ground state of the atom, respectively; $\sqrt{T_{el}/T}$ is a correction factor to allow for the difference between the temperature T of the exciting star and the electron temperature T_{el} at s (cf. Rosseland[5]); while $e^{-\tau_u}$ measures the reduction in the ionizing ultraviolet radiation due to absorption, τ_u being the optical depth from the ionizing star to the point s. Finally, w is the dilution factor at s, given by

$$w = \frac{R^2}{4s^2}. \qquad (2)$$

[4] G. P. Kuiper, O. Struve, B. Strömgren, *Ap. J.*, **86**, 570, 1937; sec. III, especially pp. 593 f. and 612.

[5] *Theoretical Astrophysics*, chap. xxii, Oxford, 1936.

We shall assume that practically all the free electrons are furnished by ionization of hydrogen, so that $N'' = N_e$. The validity of this assumption for actual interstellar space will be discussed in section V. Further, let

$$\left.\begin{aligned} N &= N' + N'' , \\ N'' &= xN , \\ N' &= (1 - x)N , \\ N_e &= xN , \end{aligned}\right\} \tag{3}$$

so that x is the degree of ionization of hydrogen. Introducing numerical values, equation (1) can now be written in the form

$$\frac{x^2}{1 - x} N = C_1 \cdot \frac{1}{s^2} \cdot e^{-\tau_u} , \tag{4}$$

with

$$\left.\begin{aligned} C_1 &= 10^{-0.51-\theta I} \cdot \frac{2q''}{q'} \sqrt{\frac{T_{el}}{T}}\, T^{3/2} \cdot R^2 , \\ \theta &= \frac{5040^\circ}{T} . \end{aligned}\right\} \tag{5}$$

The numerical factor of C_1 corresponds to the following choice of units: 1 parsec $= 3.08 \cdot 10^{18}$ cm for s; the solar radius for R; and cm^{-3} for N.

Let the absorption coefficient for the ionizing radiation per neutral hydrogen atom be a_u. We simplify the problem by assuming a_u to be independent of the frequency and equal to its value at the absorption edge. The relevant range of frequency is relatively small, so that the accuracy will be sufficient for our present purpose. Then, by definition,

$$d\tau_u = (1 - x)Na_u \cdot 3.08 \cdot 10^{18} ds , \tag{6}$$

the factor $3.08 \cdot 10^{18}$ being derived from the choice of the parsec as the unit of s.

Equations (4) and (6) define the solution of the problem of deriv-

ing the degree of ionization as a function of the distance from the star. Solving (6) for $1 - x$ and substituting in (4), we get

$$e^{-\tau_u} d\tau_u = \frac{N^2}{C_1} x^2 s^2 \cdot 3.08 \cdot 10^{18} a_u ds \,. \tag{7}$$

We introduce the following new variables:

$$y = e^{-\tau_u} \qquad (1 \geqq y > 0)\,, \tag{8}$$

$$dz = \frac{N^2}{C_1} \cdot 3.08 \cdot 10^{18} a_u \cdot s^2 ds\,, \tag{9}$$

with $z = 0$ for $s = 0$, so that

$$s = \left(\frac{3C_1}{N^2 \cdot 3.08 \cdot 10^{18} a_u} \right)^{1/3} \cdot z^{1/3}\,. \tag{10}$$

Then (4) and (7) can be written as

$$\frac{dy}{dz} = -x^2\,, \tag{11}$$

$$\frac{1 - x}{x^2} = a \frac{1}{y} z^{2/3}\,, \tag{12}$$

with

$$a = \left(\frac{9}{NC_1 \cdot (3.08 \cdot 10^{18} a_u)^2} \right)^{1/3}. \tag{13}$$

Since $\tau_u = 0$ for $s = 0$, we have, according to (8) and (10),

$$y = 1 \text{ for } z = 0\,. \tag{14}$$

In the cases of actual interest, a is a small quantity. When $a \ll 1$, it follows from (12) that, as long as y is not small compared to 1, $1 - x \ll 1$, so that x is equal to 1, very nearly. In that case it follows from (11) and (14) that

$$y = 1 - z \quad \text{for} \quad 1 - x \ll 1\,. \tag{15}$$

Consequently, when a is small, ionization is strong until z is nearly equal to 1, so that (cf. [15]) y becomes a small quantity. With increasing z the degree of ionization now decreases very abruptly, so that, for z slightly greater than 1, hydrogen is practically un-ionized.

The value of s corresponding to $z = 1$, which we shall call s_0, is, according to (10),

$$s_0 = \left(\frac{3C_1}{N^2 \cdot 3.08 \cdot 10^{18} a_u} \right)^{1/3}. \tag{16}$$

The result of the analysis can be stated as follows: for small a the ionization is nearly complete up to the distance from the ionizing

TABLE 1

x^2	s/s_0		
	$a=0.001$	$a=0.01$	$a=0.1$
1.0	0.000	0.000	0.00
0.8	1.000	0.988	0.82
0.6	1.002	1.009	0.97
0.4	1.003	1.020	1.05
0.2	1.004	1.028	1.12

star s_0, given by (16), while there is almost no ionization for distances greater than s_0.

The abrupt change of the ionization can be interpreted in the following way. Once the proportion of neutral atoms begins to increase, the absorption of the ionizing radiation increases, leading to an accelerated increase of neutral atoms. (For a somewhat more detailed discussion of this phenomenon see the investigation by the author quoted above.[4])

The exact dependence of the degree of ionization x upon the distance s from the ionizing star has been derived for three different values of a by numerical integration according to (11), (12), and (14). The results are shown in Table 1. For $a = 0.01$ the results are given in greater detail in Table 2. Finally, it may be noticed that for small a the following relation, obtained by integrating (11),

(12), and (14), putting $z = 1$, holds very nearly in the transition region between almost complete ionization and negligible ionization:

$$z = \text{Const} - a\left\{\frac{1}{1-x} + 2ln\,\frac{x}{1-x}\right\} (a \ll 1, |1-z| \ll 1) . \quad (17)$$

Numerical values of z + constant, normalized to 0 for $x^2 = 0.5$ and calculated, according to (17), as a function of x^2, are shown in Table 3. The table shows, for instance, that with $a = 0.001$ the

TABLE 2

$a = 0.01$

z	s/s_0	$y = e^{-\tau_u}$	τ_u	$1-x$	x^2
0.0	0.00	1.00	0.00	0.000	1.00
0.2	0.58	0.80	0.22	.004	0.99
0.4	0.74	0.60	0.50	.009	0.98
0.6	0.84	0.41	0.89	.017	0.97
0.8	0.93	0.22	1.52	.037	0.93
0.9	0.97	0.13	2.06	.064	0.88
1.0	1.00	0.046	3.07	.15	0.72
1.1	1.03	0.0018	6.3	0.67	0.11

TABLE 3

x^2	z+Constant Normalized to 0 for $x^2=0.5$	x^2	z+Constant Normalized to 0 for $x^2=0.5$
0.1	$+5.3a$	0.6	$-1.7a$
.2	3.8	.7	4.2
.3	2.6	.8	8.6
.4	$+1.3$	0.9	-20.1
0.5	0.0		

change from $x^2 = 0.5$ to $x^2 = 0.1$ takes place for a change in z equal to 0.0053, corresponding to a change in s of about one-sixth of 1 per cent.

For small a the relative extent of the transition region is proportional to a. From (13) and (16) it follows that as_0 is independent of C_1, i.e., of the properties of the ionizing star. Therefore, as long as a is small, the absolute width of the transition region does not vary with the properties of the ionizing star.

Combining equations (5) and (16), we find

$$\log s_0 = -6.17 + \tfrac{1}{3}\log\left(\frac{2q''}{q'}\sqrt{\frac{T_{el}}{T}}\right) - \tfrac{1}{3}\log a_u - \tfrac{1}{3}\theta I + \tfrac{1}{2}\log T + \tfrac{2}{3}\log R - \tfrac{2}{3}\log N\,. \qquad (18)$$

This relation holds for any element. Introducing the proper numerical values for hydrogen, viz., $q''/q' = \frac{1}{2}$, $I = 13.53$ volts, and $a_u = 6.3 \cdot 10^{-18}$ cm^{-2}, we get

$$\log s_0 = -0.44 + \tfrac{1}{3}\log\left(\sqrt{\frac{T_{el}}{T}}\right) - 4.51\theta + \tfrac{1}{2}\log T + \tfrac{2}{3}\log R - \tfrac{2}{3}\log N\,. \qquad (19)$$

Table 4 gives $\log s_0$ for hydrogen for $R = 1$ and $N = 1$ as a function of T. The temperatures have been so chosen as to correspond to the spectral types from O5 to B5, according to the temperature

TABLE 4

Sp.	log T	θ	log s_0 for $R=1$ and $N=1$	s_0	log a for $R=1$ and $N=1$
O5	4.90	0.063	1.73	54 parsecs $\times R^{2/3}N^{-2/3}$	7.46−10
O6	4.80	.079	1.60	40	7.59
O7	4.70	.100	1.46	29	7.73
O8	4.60	.126	1.29	20	7.90
O9	4.50	.158	1.10	13	8.09
B0	4.40	.200	0.86	7.2	8.33
B1	4.36	.219	0.75	5.6	8.44
B2	4.31	.245	0.62	4.2	8.57
B3	4.27	.269	0.49	3.1	8.70
B4	4.23	.295	0.35	2.2	8.84
B5	4.19	0.324	0.20	1.6	8.99

scale recently derived by Kuiper.[6] In making the calculation the factor T_{el}/T has been put equal to 1. With $T_{el}/T = \frac{1}{4}$ (cf. Rosseland[5]), all values of $\log s_0$ would have to be decreased by 0.10, which would correspond to a decrease of the s_0-values of 21 per cent. Table 4 also gives a according to (13) for $R = 1$ and $N = 1$; a is proportional to $R^{-2/3}$ and to $N^{-1/3}$.

For any given temperature of the ionizing star, s_0 increases with

[6] *Ap. J.*, **88**, 429, 1938.

the stellar radius R as $R^{2/3}$. If a region of interstellar space is ionized by a cluster of n similar stars, close together, then s_0 has to be calculated with an equivalent R equal to $n^{1/2}R$. This follows immediately from equation (2) for the dilution factor w. Consequently, s_0 for such a cluster is equal to $n^{1/3}$ times s_0, calculated for the individual star in the cluster. This may also be expressed by saying that the volume of interstellar space ionized by a cluster of stars close together is equal to the sum of the individual volumes that would be ionized by the stars if placed so far apart in interstellar space that the volumes did not overlap.

Table 5 gives s_0 for main-sequence stars of spectral types O5–B5. The assumed visual magnitudes[7] from which R was computed, using

TABLE 5

Sp.	T	M_{vis}	s_0
O5	79,000°	$-4^m.2$	140 parsecs$\times N^{-2/3}$
O6	63,000	−4.1	110
O7	50,000	−4.0	87
O8	40,000	−3.9	66
O9	32,000	−3.6	46
Bo	25,000	−3.1	26
B1	23,000	−2.5	17
B2	20,000	−1.8	11
B3	18,600	−1.2	7.2
B4	17,000	−1.0	5.2
B5	15,500	−0.8	3.7
Ao	10,700	+0.9	0.5

Kuiper's bolometric corrections,[6] are also given. The values of R range from about 4 to 7 solar radii. An increase in brightness of 1 mag. would lead to an increase of s_0 by a factor of 1.36.

The increase in the ionized volume as one passes from low-temperature stars to high-temperature stars is so pronounced that it may be concluded that the total volume ionized by all high-temperature stars (hotter than about B2) is much larger than that ionized by all low-temperature stars, in spite of the much greater number of the latter. For instance, one O7 star ionizes a volume equal to that ionized by about two thousand B3 stars or by about five million Ao stars.

[7] R. Trumpler, *Lick Obs. Bull.*, No. 420, 1930.

In deriving the values given above, certain simplifying assumptions have been made. The effect of a possible decrease of the factor $\sqrt{T_{el}/T}$ has already been discussed. A resulting decrease of the s_0-values on this account by more than, say, 20–30 per cent is not very probable. It has also been pointed out that a certain mean value of a_u, taken over the relevant frequency range of the ionizing radiation, should have been used instead of a_u at the absorption edge. It is estimated that this effect will lead to an increase of s_0 of probably less than, say, 20–30 per cent. Finally, the ionizing radiation emitted by the interstellar hydrogen has been neglected in calculating the ionization. An upper limit to the change of s_0 resulting from this effect is obtained in the following manner. Upon absorption of a quantum of ionizing radiation by an interstellar hydrogen atom there may follow reradiation of a quantum of the same frequency through a capture process to the ground state. In the case of hydrogen under the general conditions in question it is known that about one-third of the captures of free electrons by ions are to the ground state, the rest being to excited states. Therefore, about two-thirds of the absorption processes from the ground state are effective in removing entirely the quantum of ionizing radiation. The remaining one-third of the absorption processes also act to reduce the resulting ionization, through the scattering involved. The upper limit referred to is obtained by neglecting the effect of the scattering, thus introducing an effective absorption coefficient equal to $\frac{2}{3}\, a_u$ in (16). The maximum influence is therefore an increase of about 15 per cent in s_0. Altogether, it is estimated that the s_0-values calculated are sufficiently accurate for a first survey of the problem. It would not, however, present very great difficulties to develop a theory that would take the effects mentioned more accurately into account.

We have tacitly assumed that ionization by electron collisions is unimportant compared with photo-ionization. The justification for this assumption lies in the fact that, in interstellar space, the radiation from the ionizing stars is the primary energy source. Without making detailed calculations, we assume that any tendency for collisional ionization to become of importance is checked by a corre-

sponding decrease of the electron temperature. The mean free path of the electrons is so small as not to interfere appreciably with such an adjustment of the electron temperature.

Applications of the theory developed in this section are given in sections IV and V.

III

We shall consider in this section the problem of the excitation of the higher energy-levels of hydrogen in interstellar space. We shall limit ourselves mainly to the consideration of the level $n = 3$, which determines the emission of $H\alpha$ radiation. The discussion is naturally divided into two parts, dealing with ionized and nonionized regions, respectively.

In the almost completely ionized region surrounding a high-temperature star or a cluster of such stars, the mechanisms of excitation of one of the higher levels—say $n = 3$—can be classified as follows, leaving out of consideration mechanisms that are entirely negligible: (*a*) capture of a free electron by an ion to the state considered; (*b*) capture of a free electron by an ion to a higher state, followed by one or more transitions leading through the state considered; (*c*) Lyman-line absorption from the ground state to the state considered, and Lyman-line absorption from the ground state to higher states, followed by one or more transitions leading through the state considered; (*d*) Balmer-line absorption from the state $n = 2$, either directly to the state considered or to a higher state followed by cascading, as before; and (*e*) excitation by electron collision from the ground state to the state considered or to higher bound states, followed by cascading.

In investigating these mechanisms we can largely make use of the results of investigations of the analogous problem in the case of planetary nebulae.

Consider first mechanism (*a*). The effective cross-section $\pi\sigma^2(n)$ for capture of a free electron of kinetic energy E_e to the state with quantum number n of hydrogen is given by a well-known formula (cf., e.g., Cillié[8]) which follows immediately from the Sugiura-

[8] *M.N.*, **92**, 820, 1932; **96**, 771, 1936.

Gaunt formula for the continuous absorption cross-section and the Milne relation between continuous absorption cross-section and capture cross-section for reverse processes:

$$\sigma^2(n) = 1.43 \cdot 10^{-33} \frac{g}{n} \frac{\nu_0}{\nu} \frac{1}{E_e}, \tag{20}$$

where g is the Gaunt correction factor, which is approximately equal to 1 ($g = 0.91$ for $n = 3$), while ν_0 and ν are the frequency of the absorption edge and of the radiation emitted at the capture, respectively (so that $h\nu = h\nu_0 + \chi_n$, when χ_n is the binding energy of the state considered).

With the aid of the well-known gas-kinetic formula, giving the number of captures corresponding to a given capture cross-section (cf., e.g., Fowler[9]), and using the mean lifetimes for the various states of hydrogen, as tabulated, for example, by Bethe,[10] the number of atoms per unit volume N_n in any state n can now be calculated easily (cf. Cillié[8]). For $n = 3$ one finds

$$\frac{N_3}{N'' N_e} = 6.3 \cdot 10^{-20} \cdot T^{-1/2} \cdot J \text{ (excitation by mechanism [}a\text{] only).} \tag{21}$$

Here J denotes the proper mean value of the factor ν_0/ν^- in (20). For very small temperatures, J is approximately equal to 1; for $T = 5000°$, $J = 0.81$; for $T = 20{,}000°$, $J = 0.57$; and for $T = 50{,}000°$, $J = 0.40$.

It may be noted that, in the particularly simple case of excitation by mechanism (a) there is no difficulty at all in treating the substates of the state with $n = 3$ separately. When this is done, the numerical factor in (21) is increased by a factor of about 1.5, the number N_3 being so defined that the actual number of transitions to the state $n = 2$ is given by the product of N_3 and the standard transition probability τ_{32}, obtained by averaging according to the statistical weights.

The case of excitation by both mechanisms (a) and (b) has been

[9] *Statistical Mechanics*, Cambridge, England, 1936.

[10] *Handb. d. Phys.*, **24**, 1, chap. iii, 1933.

treated by Menzel and by Menzel and Baker.[11] These authors give the ratio $N_n/N''N_e$ in terms of the corresponding ratio for thermodynamical equilibrium. In thermodynamical equilibrium we have

$$\frac{N_3}{N''N_e} = 10^{-14.44+1.50\theta} \cdot T^{-3/2} \text{ (thermodynamical equilibrium).} \quad (22)$$

In the case of excitation by mechanisms (*a*) and (*b*)

$$\left.\begin{aligned} \frac{N_3}{N''N_e} &= b_3^{(A)} \cdot 10^{-14.44+1.50\theta} \cdot T^{-3/2} \\ &\text{(excitation by mechanisms [}a\text{] and [}b\text{]),} \end{aligned}\right\} \quad (23)$$

where $b_3^{(A)}$ is tabulated by Baker and Menzel[11] (their hypothesis A_2) as a function of the electron temperature T_{el}. The values of N_3 given by (23) are naturally larger than those given by (21). For $T_{el} = 5000°$ the increase is given by a factor about equal to 2; with increasing temperature the factor tends toward 1.

The case of excitation by mechanisms (*a*), (*b*), and (*c*) has been considered by Cillié[8] and by Menzel and Baker.[11] Following Zanstra,[12] they treated the case in which the exciting Lyman-line radiation, as well as the ionizing radiation, which determines the relative number of atoms in the ground state (from which the excitation considered takes place), is given by a common dilution factor times the Planck intensities for a common temperature. In this case the transitions from any excited state to the ground state are exactly balanced by the reverse Lyman-line excitations, and the treatment is analogous to the treatment of the case (*a*) + (*b*), except that all transition probabilities to the ground state are put equal to zero.

In the particular case of excitation by mechanisms (*a*), (*b*), and (*c*) just considered,

$$\left.\begin{aligned} \frac{N_3}{N''N_e} &= b_3^{(B)} \cdot 10^{-14.44+1.50\theta} \cdot T^{-3/2} \\ &\text{(particular case of excitation by mechanisms [}a\text{],[}b\text{], and [}c\text{]),} \end{aligned}\right\} \quad (24)$$

[11] D. H. Menzel, *Ap. J.*, **85**, 330, 1937; D. H. Menzel and J. G. Baker, *Ap. J.*, **86**, 70, 1937; J. G. Baker and D. H. Menzel, *Ap. J.*, **88**, 52, 1938.

[12] *Pub. Dom. Ap. Obs., Victoria*, **4**, 200, 1931; *Zs. f. Ap.*, **2**, 1, 1931.

where $b_3^{(B)}$ is tabulated by Baker and Menzel (their hypothesis *B*) as a function of the electron temperature.

With regard to the importance of excitation by mechanism (*d*), we shall only consider two limiting cases. If the excitation of the state $n = 2$ is normal for interstellar space, the role of mechanism *d* is entirely negligible. If, however, the excitation of the state $n = 3$ is supernormal to such an extent that the ionized region becomes opaque in the frequencies of the Balmer lines, then the relative population of the state $n = 3$, excited by mechanisms (*a*), (*b*), (*c*), and (*d*), approaches the value given by expression (22), valid for thermodynamical equilibrium, with the temperature about equal to that of the ionizing star. (For the possibility of superexcitation of the state $n = 2$, owing to the metastability of the 2*s*-substate, see Chandrasekhar and Stoy, as quoted by Cillié.[8])

With regard, finally, to the importance of excitation by mechanism (*e*), it is easily seen that in an almost completely ionized region, and for temperatures of the order of those to be expected in actual applications to problems of interstellar space, the mechanism is unimportant. The average capture cross-section for the capture of a free electron by an ion, to the state $n = 3$, will, for the temperatures in question, be of the order of magnitude 10^{-21}. The cross-section for excitation by an electron of a neutral atom in the ground state to the state $n = 3$ is of the order of magnitude 10^{-17}, if the energy of the electron is high enough to excite the state $n = 3$ at all. The fraction of electrons that have sufficient energy for excitation is of the order of magnitude 10^{-3}. When, as in the case under consideration, the ionization is so high that the number of ions is, say, 10^2–10^4 times the number of neutral atoms, then mechanism (*e*) will be unimportant compared with mechanisms (*a*) and (*b*).

It is interesting to note, as can easily be shown, that even in such cases of less complete ionization, when mechanism (*e*) is of importance, the ratio $N_3/N''N_e$ will approach the value given by equation (23), the reason being that, for high-level states like $n = 3$, the cross-section for electron ionization from the ground state is considerably larger than the cross-section for electron excitation of that particular state from the ground state (cf. Bethe[10]). In interstellar space, moreover, we assume that electron ionization is unimportant com-

pared with photo-ionization as a consequence of an adjustment of electron temperature. This effect also limits the importance of mechanism (*e*) in the case considered.

Table 6 illustrates equations (21), (22), (23), and (24), valid for the various cases considered. However, the table does not give the ratio $N_3/N''N_e$ directly. It gives, with a view to the application in the following section, the value of N_e, calculated with $N'' = N_e$ and $N_3 = 3 \cdot 10^{-21}$. For other values of N_3, N_e may be obtained by

TABLE 6*

θ	T	(1) Thermodynamical Equilibrium; Special Case of Excitation $(a)+(b)+(c)+(d)$	(2) Special Case of Excitation $(a)+(b)+(c)$ (Eq. [24])	(3) Excitation $(a)+(b)$ (Eq. [23])	(4) Excitation (a) (Eq. [21])	(4′) Excitation (a); Substates Considered Separately
1.0	5,040°	0.10 cm^{-3}	1.0 cm^{-3}	1.4 cm^{-3}	2.0 cm^{-3}	1.7 cm^{-3}
0.8	6,300	0.16	1.1	1.6	2.2	1.8
0.6	8,400	0.28	1.2	1.8	2.4	2.0
0.4	12,600	0.55	1.4	2.2	2.8	2.3
0.2	25,200	1.3	2.0	3.0	3.8	3.1
0.1	50,400	2.5	2.8	4.3	5.2	4.2

* The table gives N_e for $N'' = N_e$ and $N_3 = 3 \cdot 10^{-21}$ cm^{-3}.

multiplication with the square root of the factor by which N_3 differs from $3 \cdot 10^{-21}$.

It is interesting to note that for the whole range of excitation mechanisms considered, and also for the relevant range of temperatures, the values of N_e come out approximately the same. (As was noted above, in the special case of excitation $[a] + [b] + [c] + [d]$ the temperature approaches the temperature of the ionizing star, so that the relatively small numbers in the upper left corner of Table 6 are irrelevant. For mechanism $[a] + [b]$, say, the temperature in question is the electron temperature, and so may be considerably lower than that of the star; but here the change in the temperature affects N_e very little.) The relative insensitivity of the ratio $N_3/N''N_e$ here encountered is not surprising. We may mention the analogous example of the approach of the central intensities of stellar

absorption lines to the value for thermodynamical equilibrium, for temperatures high compared with the binding energy.

Further, it is of interest to note that for mechanisms (*a*), (*b*), (*c*), and their combinations the ratio $N_3/N''N_e$ is independent of the distance from the ionizing star. This is not true for mechanism (*e*), which, however, as we have seen, is unimportant in the present connection.

We shall now consider briefly the actual mechanism of excitation in the ionized regions around the high-temperature stars. The problem is not quite simple, but it is suggested that, in the major part of the ionized region, Lyman-line radiation is present almost only in the form of $L\alpha$, the radiation in the other Lyman lines having been converted by repeated fluorescence processes into $L\alpha$, Balmer lines, Paschen lines, etc.; also, that the ionized region is transparent in the frequencies of the Balmer lines (cf. above), so that the excitation of the state $n = 3$ and of higher states is by mechanism (*a*) + (*b*) (Table 6, case 3).

In the paper quoted at the beginning of this article, Struve[2] calculated the ratio $N_3/N''N_e$ in an ionized region of interstellar space by a procedure leading to equation (22) (Table 6, case 1), namely, the use of the Boltzmann and the Saha formulae with a common dilution factor which drops out in forming $N_3/N''N_e$. It follows from the previous discussion that the value of the ratio obtained by Struve will not differ very much from those obtained on any of the other hypotheses discussed. The improved method for calculating $N_3/N''N_e$ briefly outlined by Struve is essentially equivalent to that used here in case 3, i.e., the case which probably corresponds most closely to actual conditions.

We finally have to discuss the excitation of hydrogen in the practically un-ionized regions considered in section II. Nearly all the radiation beyond the Lyman limit, and also that in the Lyman lines $L\beta$, $L\nu$, etc., has here been converted into $L\alpha$ and low-frequency lines. Free electrons, supplied by elements of lower ionization potential than hydrogen, will all have relatively low kinetic energy. Therefore, in these parts of interstellar space there is almost no excitation of the state $n = 3$ or of higher states. The state $n = 2$ is probably superexcited by a factor of 10^3, very roughly, owing to the

conversion of continuous radiation into La, while the metastability of the substate $2s$ is of no consequence here.

Eddington[3] has suggested that hydrogen in un-ionized regions of interstellar space is present in molecular form. It is not intended to attempt a complete solution of this problem here, but a few points may be noted. If the equilibrium between hydrogen atoms and molecules is determined principally by one process and its reverse process, the ratio of atoms to molecules will be given by an equation analogous to (1). (In interstellar space the lowest vibrational and rotational level only will be excited. The reduced mass $\frac{1}{2}m_H$ occurs instead of m_e, however.) If the frequency of the radiation absorbed in the dissociation process considered were less than that of the Lyman limit, the factor corresponding to $e^{-\tau_u}$ would be of the order of magnitude 1. In that case the ratio of molecules to atoms would be, roughly, $10^{-9}N$; i.e., the number of molecules would be negligibly small. If, however, the frequency of the dissociation process is greater than that of the Lyman limit—and this is certainly the case if the dominant dissociation and recombination processes are the same as in the laboratory—then the number of dissociations is practically zero. On the other hand, the reverse recombination process, which involves the collision of one normal and one excited hydrogen atom, is extremely slow in interstellar space. Using the approximate value for the effective cross-section of this process given by Terenin and Prileshajewa[13] and by Rompe,[14] namely, 10^{-5} times the gas-kinetic cross-section, it is found that every hydrogen atom collides to form a molecule once in (very roughly) 10^{21} years. This means that molecule formation during any accepted time-scale is negligible. This, of course, does not definitely settle the question. It should be added that the mixture of material in the galactic system will tend ultimately to bring any molecules that may exist into ionized regions, where they will quickly dissociate. A sufficiently strong mixture will thus lead to practically complete dissociation of molecules into atoms.

IV

According to the analysis of the preceding sections, one would expect—if the density of interstellar hydrogen is within a certain range

[13] *Phys. Zs. Soviet Union*, **3**, 337, 1932. [14] *Phys. Zs.*, **37**, 807, 1936.

—to find Balmer-line emission limited to certain rather sharply bounded regions in space surrounding high-temperature stars or clusters of high-temperature stars, the emission being of uniform strength, without any concentration toward particular stars, within these regions. With a view to the relative ionizing efficiency of O and B stars, as discussed in section II, one would identify the high-temperature stars in question principally with O stars.

Comparing this picture with the observations by Struve and Elvey,[1] referred to at the beginning of this article, of extended regions of *Hα* emission, it is tempting to interpret the observed areas of uniform *Hα* emission as the projections of bounded regions of interstellar space ionized principally by clusters, or condensations, of O stars. We shall, for the present, accept this interpretation as a working hypothesis.

Our working hypothesis may be regarded as a specialized version of the more general hypothesis put forward by Struve[2] in the investigation previously referred to.

Several clusters or clusterings of O stars are known.[15] In accordance with our working hypothesis we connect the observed extended *Hα* emission region in Cygnus with the cluster of O stars having its center at $l_g = 42°$, $b_g = +1°$. About ten of the known O stars presumably belong to this cluster. Likewise, we connect the extended *Hα* emission in Cepheus with the condensation of O stars around galactic longitude 70°.

We can now immediately make use of the analysis of section III to derive the density of interstellar hydrogen in the regions in question. Struve[1, 2], from the observed strength of the *Hα* emission in Cygnus and Cepheus, derived $N_3 = 3 \cdot 10^{-21}$ cm^{-3}, assuming the effective length of the emitting column to be 1000 parsecs. Using this number we estimate, with the aid of Table 6, that the density N of hydrogen is equal to 2–3 cm^{-3}. We have here assumed that practically all the free electrons result from hydrogen ($N'' = N_e$, and also $N'' = N$, the ionization being nearly complete). This is probable a priori and is further supported by reasons stated below. With an estimated depth of the emitting column of 300 parsecs,

[15] C. H. Payne, "The Stars of High Luminosity," *Harvard Obs. Monograph*, No. 3, chap. vi, Cambridge, Mass., 1930; J. S. Plaskett, *Pub. Dom. Ap. Obs., Victoria*, **2**, 339, 1924; O. Struve, *A.N.*, **231**, 17, 1927.

instead of 1000 parsecs, one would find N equal to about 4 cm^{-3}. The resulting N is proportional to the square root of the assumed value of N_3.

Assuming, for the present, that $N = 3$, we find, with the aid of Table 5, that the diameter of the region ionized by a cluster of n stars of the average spectral type O7 is about 80 $n^{1/3}$ parsecs. With $n = 10$ (cf. above) we find a diameter of about 200 parsecs. This agrees about as well as could be expected with the estimated diameter of the Cygnus emission regions of, say, 200–300 parsecs.

The total intensity of a hydrogen-line emission area is proportional to the number n of ionizing O stars. The total area is proportional to $n^{2/3}$, the depth, and hence the surface intensity, to $n^{1/3}$.

With regard to the extension of the areas of $H\alpha$ emission in the direction at right angles to the galactic plane, consideration of the concentration of hydrogen toward the galactic plane is of importance. Calculations based on the assumption of a static interstellar hydrogen cloud may perhaps serve as a rough guide. Using the empirical field of force in the direction at right angles to the galactic plane as derived by Oort,[16] it is found that the density of hydrogen decreases with the height above the galactic plane approximately according to a Gaussian error law, with a dispersion of about 1.3 parsecs $\times$ $T^{1/2}$, where T is the temperature of the hydrogen gas. With $T = 10{,}000°$, a dispersion of 130 parsecs results. Though the true distribution will probably differ from this, owing to the effects of turbulence, the order of magnitude should be correct.

It is, of course, very important to find how large a fraction of the relevant galactic stratum of hydrogen is ionized. From the estimated density of O and B stars, in connection with Table 5, assuming $N = 3$ cm^{-3}, we are led to the very rough estimate that about one-tenth of the stratum is ionized. The numerical value of the fraction is inversely proportional to the square of the density of interstellar hydrogen.

As the observational material on extended areas of hydrogen-line emission accumulates, it will be possible to test the working hypothesis formulated in this section. The necessity of a critical test is obvious, particularly in view of the fact that a revision of the temperature scale might lead to a somewhat different picture of the relative

[16] *Bull. Astr. Inst. Netherlands*, **6**, 249, 1932.

importance of O and B stars and that a decrease in the accepted value of N might lead to a less pronounced separation between ionized and nonionized regions.

Further observations of hydrogen-line emission areas would be especially valuable, as they would lead to an improved knowledge of the relative extent of that part of the galactic stratum in which hydrogen is ionized.

At the present moment it can be said that a number of determinations, or estimates, of the density of interstellar hydrogen lead to values in approximate mutual agreement. First, Dunham's[17] discovery of interstellar lines of neutral calcium and the discussion of this phenomenon by Dunham and Struve suggest as the most plausible choice of the value of the hydrogen density the maximum value compatible with the results of Oort's dynamical investigations, i.e., $N = 2$–4 cm^{-3} (cf. Struve[2]). The analysis based upon the strength of interstellar $H\alpha$ emission leads to a value of N around 3 cm^{-3}. The observed extent of $H\alpha$ emission areas confirms the approximate correctness of this value. Finally, it may be mentioned that Eddington's estimate, based upon the average separation of nebular condensations, when modified to correspond to a mean molecular weight of 1, leads to $N = 5$ cm^{-3}.

V

We shall consider briefly the state of ionization of elements other than hydrogen. In those regions of interstellar space where hydrogen is ionized, the electron density N_e is equal to N. All ionizing radiation of wave lengths shorter than that of the Lyman limit comes from stars within the ionized region, i.e., particularly from the same stars which ionize the hydrogen. This radiation is not very much reduced by hydrogen absorption except near the boundary of the ionized region (cf. sec. II). In the case of sufficiently abundant elements of high ionization potential the ionization may be checked in a way analogous to that in which the ionization of hydrogen is checked. With obvious modification, the analysis in section II holds for such cases. Thus, it is seen that, if helium were as abundant as, or more abundant than, hydrogen, ionized helium would be restricted to a volume considerably smaller than that of ionized hydrogen. If, on the other hand, helium is considerably less abundant than hydro-

[17] *Pub. A.S.P.*, **49**, 26, 1937; *Nature*, **139**, 246, 1937.

gen, the ionization of *He* I to *He* II will usually be almost complete up to the boundary of the region of hydrogen ionization; but in that case, of course, helium contributes considerably less to the number of free electrons than hydrogen. This argument tends to confirm the validity of our assumption that the free electrons are contributed mainly by hydrogen in those regions where hydrogen is ionized. It also shows that helium D_3-line emission is handicapped in comparison with hydrogen Balmer-line emission.

Struve and Elvey[1] observed the emission line λ 3727 of [*O* II] in many of the areas where *Hα* was seen, while N_1 and N_2 of [*O* III] were rarely observed. As the mechanism of excitation of the lines is similar, this probably indicates that oxygen is present mainly as *O* II. Further observations on the occurrence of N_1 and N_2 may lead to valuable results, particularly so if it should turn out that the abundance of oxygen is high enough to restrict the ionization of *O* II to *O* III (ionization potential 34.9 volts) by a mechanism similar to the hydrogen mechanism.

Ultimately, the observed relative intensity of interstellar hydrogen and oxygen emission lines will lead to a reliable value of the relative abundance of interstellar hydrogen and oxygen. A very rough estimate is easily made. The effective cross-section for the excitation of the upper state of λ 3727 by electron collision is estimated to be somewhat smaller than 10^{-17} cm². Assuming that somewhat less than one-tenth of the electrons have sufficient energy to excite λ 3727, and putting the cross-section for capture of a free electron to the state $n = 3$ equal to about 10^{-21} cm², we derive from the observed fact that λ 3727 is somewhat fainter than *Hα* that there are, roughly, 10^2–10^3 *H* ions to every *O* II ion. Since hydrogen is largely ionized, and oxygen is mostly present as *O* II, the resulting interstellar abundance is 10^{-2}–10^{-3} oxygen atoms to every hydrogen atom.

We consider next the ionization of elements with ionization potential less than that of hydrogen, in those regions where hydrogen is ionized. In this case the ionizing radiation comes from the entire galactic system, so that the customary calculations of the dilution factor and the effective temperature hold, while the electron density N_e is equal to N. It should be noted that the O stars which ionize the hydrogen do not contribute especially to the ionization of such elements as calcium and sodium.

Outside the regions in which hydrogen is ionized, there will be almost no ionization for ionization potentials larger than that of hydrogen. Of the most abundant elements, helium, nitrogen, and oxygen will be un-ionized, while carbon and the metals will be ionized. Of the abundant metals, only calcium will be doubly ionized. It may be noticed that titanium will be present mostly as *Ti* II. This is of interest in connection with Dunham's[17] observations of interstellar *Ti* II lines.

It is quite likely that in the regions of un-ionized hydrogen most of the free electrons are furnished by carbon. With an interstellar carbon abundance of the same order as the abundance derived for oxygen, we find that N_e is about 10^2–10^3 times smaller than in the regions where hydrogen is ionized. This figure is, however, as yet extremely uncertain. It is probably best to postpone the detailed discussion of the ionization of the metals until two basic constants are known with greater certainty, namely, the fraction of the galactic stratum in which hydrogen is ionized, and the ratio of electron density in regions of ionized and un-ionized hydrogen, respectively. With the present values for these constants it is found that interstellar *Ca* I lines are almost entirely absorbed in the regions of ionized hydrogen, while *Ca* II, *Na* I, and *K* I lines are also mostly absorbed here.

Restriction of the absorption of an interstellar line to a fraction of the galactic stratum naturally affects the abundances calculated from the observed intensities of the line. Increasing the abundance of calcium and sodium found by Struve[2] (forming an average abundance of the two elements) on this account, and using $N_e = 3$ in the absorption region, we arrive at a density of 3.10^{-5} cm^{-3}. Adopting, for interstellar space, the relative cosmic abundances of oxygen, calcium, and sodium, as determined by Goldschmidt,[18] the corresponding density of oxygen is found to be 5.10^{-2} cm^{-3}. The resulting interstellar abundance is $2 \cdot 10^{-2}$ oxygen atoms to every hydrogen atom, which is of the same order as the value determined above from the strength of the line λ 3727. It is hardly necessary to emphasize the fact that some of the factors entering into this calculation will certainly need considerable revision.[19]

[18] *Norske Videnskaps-Akademi, Oslo,* Mat.-Naturv. Kl., No. 4, 1937.

[19] In a more refined calculation of the ionization of an element in interstellar space the effect of recombination processes to excited states, followed practically always by

Struve[20] has recently emphasized the relatively much greater sensitivity of the interstellar absorption-line method as compared with the interstellar emission-line method. Even so, it seems already quite clear that the emission-line method is capable of yielding, ultimately, extremely valuable results with regard to the determination of the interstellar density of the most abundant elements, all of which show no interstellar absorption lines in the accessible wavelength region.

The author is much indebted to Dr. O. Struve for placing at his disposal the results of investigations on the subject of this paper before their publication.

COPENHAGEN OBSERVATORY
February 15, 1939

---

cascading to the ground state, must be taken into account. The effect will always tend to decrease the degree of ionization. For hydrogen the effect is not very marked, leading to an extra factor on the right-hand side of equation (1) estimated to be about equal to $\frac{1}{3}$. This would correspond to a decrease of the s_0-values calculated in the present paper by about 30 per cent. For elements like sodium and potassium, however, the effect is very marked. It is well known (cf. e.g., n. 4) that for these elements the absorption from the ground state is much smaller than for hydrogen, while, according to an unpublished investigation by Mr. M. Rudkjöbing, the excited states are approximately hydrogen-like with regard to continuous absorption. It follows that for these elements the number of recombinations to excited states is far greater than the number of recombinations to the ground state. In interstellar space the number of dissociation processes is, of course, proportional to the continuous absorption coefficient for the ground state. We conclude that the degree of ionization of sodium and potassium in interstellar space is quite considerably reduced by the effect in question. The abundances of sodium and potassium calculated from the strength of interstellar absorption lines are similarly reduced. According to an unpublished result by Dr. L. C. Green, kindly communicated to the writer, *Ca* II is intermediate between sodium and hydrogen with regard to the continuous absorption from the ground state. Hence, a reduction of the calculated calcium abundance is indicated, but it is smaller than for sodium. Pending more accurate calculations, it is suggested that the remainder (cf. Struve[2]) of the well-known discrepancy with regard to the relative strength of interstellar *Na* I and *Ca* II lines will disappear when the effect just considered is taken into account. For *Ca* I the continuous absorption coefficient from the ground state has not yet been calculated. It is very probable, however, that it is considerably smaller than for hydrogen, the excited states being more hydrogen-like with respect to continuous absorption. If this is the case, it follows that the interstellar ratio of *Ca* I to *Ca* II is considerably larger than that calculated from the customary equation. This would tend to reconcile the value of the electron pressure derived from the observed strength of *Ca* I and *Ca* II (cf. Dunham[17] and Struve[2]) with that found in the present investigation.

[20] *Zs. f. Ap.*, **17**, 316, 1939.

NOTES

TWO NEW WHITE DWARFS; NOTES ON PROPER MOTION STARS

ABSTRACT

This note is a brief report on some of the observations made with the 82-inch telescope during the first month of its operation.

During the first month of regular operation the 82-inch telescope was used mainly in the determination of accurate spectral types for stars of large proper motion (not less than $0''.30$ per year). About 400 spectra were obtained for about 250 stars between visual magnitudes 8 and 16. Three classes of objects of special interest are expected to be found in such a survey: (1) white dwarfs; (2) intermediate white dwarfs or, more generally, stars not over 2 or 3 mag. below the main sequence; and (3) stars of large (spectral) parallax. It is found that the second group extends almost along the whole main sequence. Since these stars merge into the main sequence and are much more similar to main-sequence stars than to white dwarfs (probably also in the interior),[1] the name "subdwarfs" is suggested for this class of stars, in analogy with "subgiants." This name will prevent the confusion of these stars with the white dwarfs proper which are very much fainter.

During the past month two new white dwarfs were found, perhaps two dozen of subdwarfs, and more than a dozen stars with spectral parallax in excess of $0''.1$. These incidental results are not regarded as the sole object of the survey; its main purpose is the derivation of the properties of the near-by stars by completely covering the known stars of proper motion above $0''.30$. About 600 faint stars have been observed so far since the work was started last year at the Yerkes Observatory.

Table 1 contains the white dwarfs and the most probable subdwarfs found with the 82-inch telescope. In addition, most of the known white dwarfs were observed (a few objects were in inaccessible parts of the sky) and a summary of the comparisons between these objects is given below.

Wolf 457 has a color index of about zero, and has a continuous

[1] This may be seen, e.g., from Table 11, p. 508, of B. Strömgren, *Erg. d. Ex. Nat.*, **16**, 1937.

spectrum between about 6600 and 3800 A. Ross 808 has strong and broad Balmer lines and apparently belongs to that group of the white dwarfs of which 40 Eridani B is the prototype. According to the writer's observations, 8 of the white dwarfs now known belong to that group. Their spectra are almost indistinguishable and show

TABLE 1

Star	α	δ	m_{vis}	P.M.	Sp.	100π(Sp)
Wolf 457	12:55.1	+ 4:02	15.6	1".05	O	.....
Ross 808	15 57.7	+37 06	14.4	0.58	Ao	.....
Ross 338	2 51.2	+48 28	13.2	0.42	G2	0".20
Ross 585	3 24.4	+33 43	12.9	1.41	K4	0.83
Ross 600	4 35.4	+22 43	13.0	0.68	Ko	0.38
Sel. A. 342	5 09.7	+60 24	14.8	0.50	K3	0.26
Ross 49	5 39.4	+ 9 13	11.9	0.60	F8	0.29
Ross 988	7 21.5	+38 11	13.8	0.74	Ko	0.28
Ross 390	7 30.1	−10 10	11.9	0.62	G5	0.42
Wolf 1059	7 54.3	+29 18	12.6	0.53	Go	0.24
AC 78°3159	8 49.	+78 54	12.3	0.61	G8	0.46
Ross 890	9 44.5	+ 7 05	12.4	0.32	F8	0.23
Ross 892	10 22.3	+ 1 55	11.4	0.38	F8	0.36
Ross 108	11 00.3	+53 45	15.2	0.77	K6	0.46
Sel. A. 33	11 30.9	+29 24	13.8	0.88	K3	0.42
Ross 114	11 31.4	+14 57	13.8	0.53	G5	0.17
Ross 904	11 36.1	+25 39	12.9	0.47	G8±	0.35±
+26°2251	11 39.5	+26 07	10.6	0.52	F8	0.52
+51°1696	11 41.4	+51 27	9.5	1.02	Go	1.0
Ross 908	11 47.5	+28 06	12.1	0.92	G5	0.38
−4°3208	12 02.2	− 5 10	10.2	0.54	Fo	0.35
Ross 453	12 05.8	+ 0 58	11.2	0.50	Fo±	0.22±
+2°2538	12 20.5	+ 1 51	9.8	0.51	F2	0.48
Ross 974	12 56.9	− 1 33	12.5	0.57	G5	0.32
Ross 838	13 56.8	+ 9 25	11.5	0.88	G5	0.50
Ross 841	13 57.3	− 5 10	11.2	0.44	A2s	0.13

only the strong Balmer lines up to about $H\zeta$. These stars are, in order of right ascension: 1166 h Persei,[2] 40 Eridani B,[3] Hertzsprung 3 = CC 398,[4] Furuhjelm I, 182,[5] Wolf 485 = BD −7°3632,[6] Ross 808,[7]

[2] Oosterhoff, *B.A.N.*, **6**, 39, 1930. [3] Adams, *Pub. A.S.P.*, **26**, 198, 1914.

[4] Kuiper, *Pub. A.S.P.*, **49**, 341, 1937; see also Ramberg, *A.N.*, **265**, 111, 1938.

[5] Deutsch, *Observatory*, **62**, 53, 1939. The proper motion was known; the spectral class used was from the *Bergedorf Spektral Durchmusterung*.

[6] Kuiper, *op. cit.*, **47**, 307, 1935. Dr. A. van Maanen has pointed out to the writer that the co-ordinates of BD −7°3632 agree with those of Wolf 485, so that the BD designation may be used in spite of the faintness of the star, 12.0 mag.

[7] This note.

Wolf 1346,[8] and AC 82°3818.[9] In addition, the two white dwarfs in the Hyades[10] probably belong to this group. The absolute magnitude of these objects seems to be about +11; a recent parallax determination at the Cape of Wolf 485 makes the weighted mean parallax of this star $0''.064 \pm 8$, giving an absolute magnitude of +11.0, nearly the same as for 40 Eridani B, +11.2.

Ross 627[11] does show the Balmer lines, but they are much shallower than for the stars of the preceding group. This fact may be interpreted as being due to a larger surface gravity—a result of the lower absolute magnitude ($13\frac{1}{2}$–14) and probably a much smaller radius. This star forms a transition to the stars with practically continuous spectra, in which the Balmer lines have become so shallow as to be invisible. The three cases in this group, all found by the writer, are AC +70°8247,[12] Wolf 219,[13] and Wolf 457.[7] Shallow lines may exist in these spectra, but it is obvious that these spectra are unlike any found for main-sequence stars. The fact that the Balmer lines are invisible can be interpreted as the result of high surface gravity,[12] possibly also by rapid rotation. The *ad hoc* assumption that no hydrogen exists in these stars, even in the atmosphere, which as a result of excessive surface gravity may contain a much greater abundance than the star as a whole, seems very unsatisfactory in view of the great strength of the Balmer lines in the majority of the white dwarfs. (The theoretical difficulty with the energy generation is not serious unless it is shown that there is a thorough mixing of the elements throughout the star; on the contrary, this very difficulty points to the opposite in connection with the strong Balmer lines in the majority of the white dwarfs.)

In addition, five other white dwarfs are known: the companion to Sirius (A5),[14] that to Procyon (spectrum unknown),[15] van Maanen

[8] Kuiper, *op. cit.*, **46**, 290, 1934. [9] *Ibid.*, **47**, 279, 1935.

[10] One was suspected by Schwassmann and van Rhijn, *M.N.*, **94**, 517, 1934. This was confirmed and another added by Ramberg in *A.N.*, **265**, 111, 1938.

[11] Humason and van Maanen, *Pub. A.S.P.*, **48**, 179, 1936.

[12] *Op. cit.*, **47**, 307, 1935.

[13] *Ibid.*, p. 96, 1935. The writer has not yet been able to observe this star with the 82-inch telescope, but Mr. Humason, of the Mount Wilson Observatory, has informed him that he found Wolf 219 to have a continuous spectrum.

[14] Adams, *Pub. A.S.P.*, **27**, 236, 1915. [15] E.g., *Ap. J.*, **88**, 490, 1938.

2 (G0; actually the spectrum differs from any type applicable to ordinary dwarfs),[16] Wolf 489,[17] and Ross 451.[17]

Wolf 489, with absolute magnitude about 15.1 visually, 15.8 photographically, as derived at Mount Wilson, is perhaps the most peculiar of the white dwarfs. At the Yerkes Observatory its spectrum was found to be earlier than M; later (unpublished) it was found not to be of type K. Two spectra obtained with the 82-inch telescope, covering the region between 3800 and 6600 A, fail to show any lines, although the intensity distribution is clearly in agreement with the approximate value of the color index derived (about 0.7 mag.). The most amazing fact is the absence of the H and K lines which would be expected to be the strongest lines in the spectrum. The presence of faint traces of these (and other) lines is, of course, not precluded, but it is certain that none of the strong features used in the Draper classification or used for classification in the visual region is present in anything approaching their normal strength. The color index of the star will be determined more precisely in order to obtain a good determination of the radius of the star.

Ross 451 (K4) is thus the latest among the white dwarfs; but since it seems to be only between 3 and 4 mag. below the main sequence, it might perhaps more properly be considered a subdwarf. Further determinations of its parallax will be important in this connection.

The probable subdwarfs in Table 1 are selected mainly on the basis of abnormally high transverse motion computed under the assumption of the star being a normal dwarf. If the proper motion is one hundred times the spectral parallax or more, the star is probably below the main sequence. In some cases the ratio is about 300; then, even if the transverse motion is as high as 474 km/sec, the star must be over 2 mag. below the main sequence. Actually small observational errors will make the distinctions less precise, and some of the stars can only be presented as probable cases. There is, however, an additional criterion for identifying these subdwarfs for types earlier than about G5: the weakness of the Balmer lines and the G band. A more extensive discussion of these stars will be published later.

One new double star was found among the near-by stars: $+10^{\circ}$

[16] Seares, *Pub. A.S.P.*, **30**, 191, 1918. [17] Kuiper, *Ap. J.*, **87**, 593, 1938.

1857, $9^m.5$, K6+; separation 2″, $\Delta m = 3.5$. The star has a third component, separation 115″, $12^m.2$, M4+. The spectral parallax of the system is 0″.08.

G. P. KUIPER

McDONALD OBSERVATORY
April 1939

THE BEHAVIOR OF *He* I λ 5015 IN ζ TAURI AND φ PERSEI

ABSTRACT

The *He* I line λ 5015 ($2^1S - 3^1P$), predicted to be sharp in ζ Tauri and φ Persei, as a result of dilute radiation in the nonrotating outer shells of these stars and the metastability of the 2^1S level, is found to be as broad as D_3 in ζ Tauri and absent or present only as a very faint, broad line in φ Persei.

In a recent paper on excitation phenomena in outer shells of stars Struve and Wurm[1] explain the observed strength and sharpness of the *He* I line λ 3965 ($2^1S - 4^1P$) in ζ Tauri (B3e) and φ Persei (Bone) as being due to the metastability of the 2^1S level and to the presence of nonrotating outer shells. Dilute radiation presumably causes the 2^1S level to become richly populated with respect to the higher nonmetastable levels, thus accounting for the strength of the line, while its sharpness is considered a result of the nonrotating shell. The corresponding lines arising from the photosphere, presumed to be rotating rapidly, are greatly broadened and indistinct but bear the expected relative intensities as a consequence of the absence of dilute radiation.

The only other available line arising from the 2^1S level is λ 5015 ($2^1S - 3^1P$). It was not observed by Struve and Wurm, owing to its presence in the green part of the spectrum, but it was assumed that it would behave similarly to λ 3965.

Two plates in the visual region of ζ Tauri (October 5 and December 24, 1936) and one of φ Persei (September 22, 1937), taken by Dr. Cherrington with the Yerkes auto-collimating grating spectrograph (27 A/mm), were available in the files of spectrograms at the Perkins Observatory. Plate XXV shows λ 5015 and D_3 in (*a*) ζ Tauri and (*b*) φ Persei. Microphotometer tracings of these regions are shown immediately below.

Inspection shows that in ζ Tauri λ 5015 appears as broad as D_3

[1] *Ap. J.*, **88**, 84, 1938.

PLATE XXV

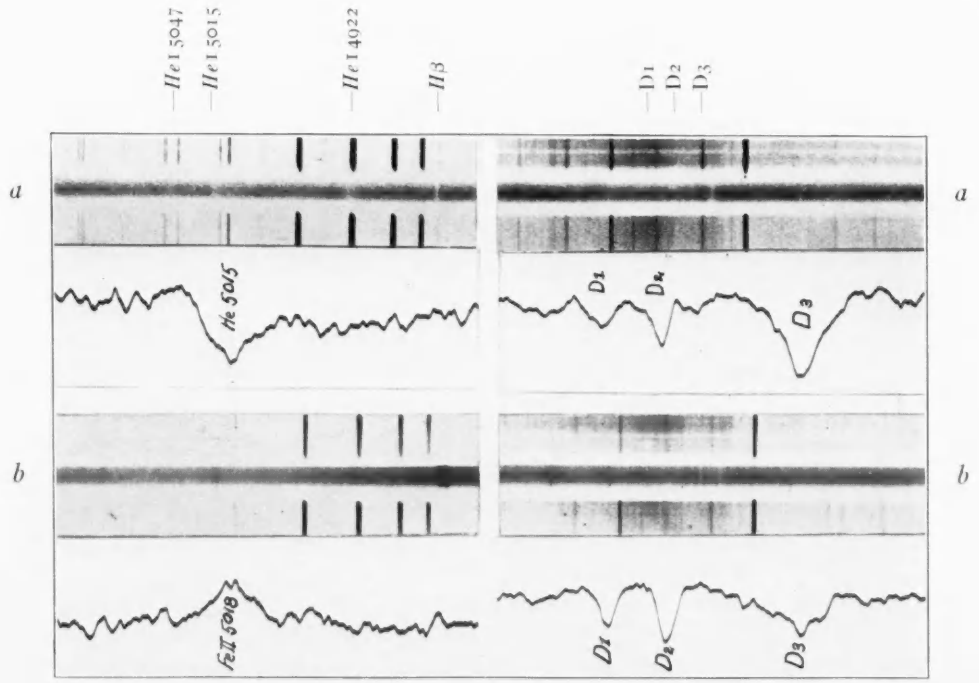

a) ζ TAURI; *b*) φ PERSEI

The scale of the tracings is six times larger than the scale of the spectra

PLATE XXVI

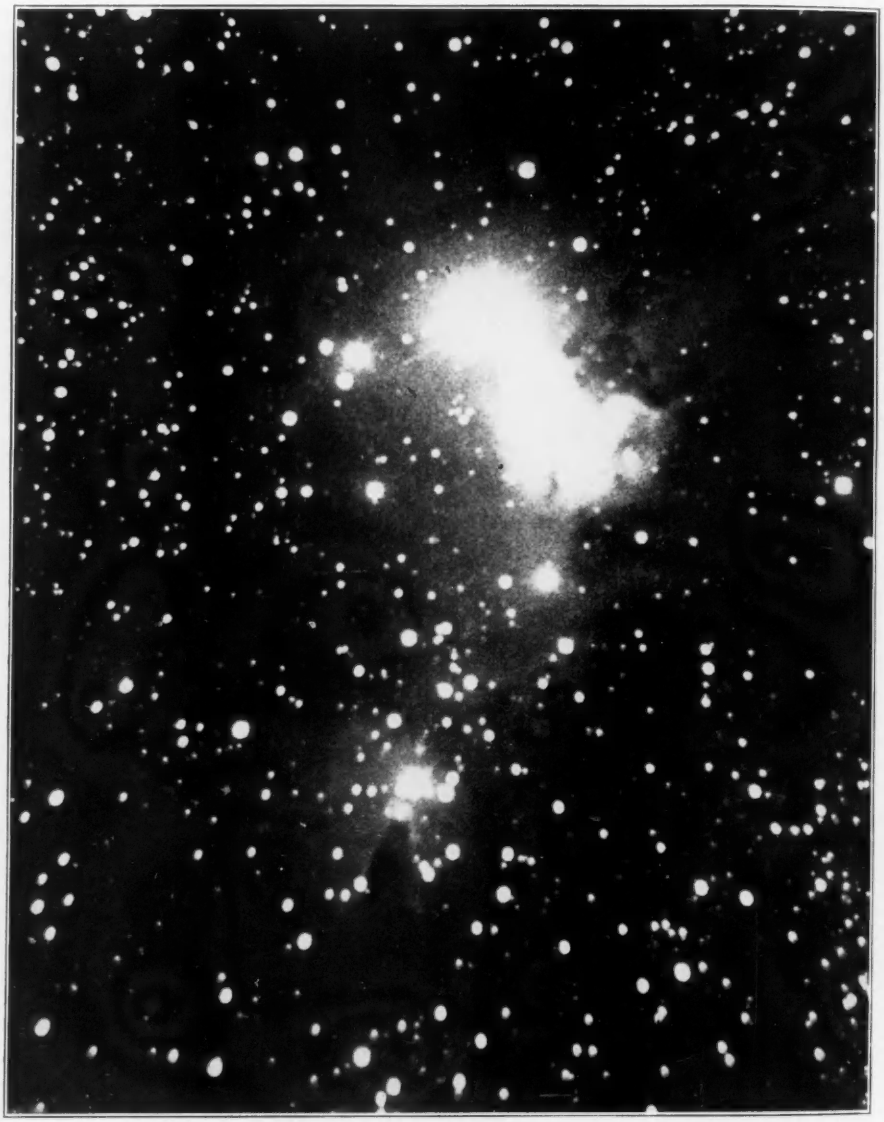

THE BRIGHT NEBULOSITY SOUTH OF S MONOCEROTIS

of *He* I and that λ 4922 and λ 5047 are present and have similar profiles to that of λ 5015. The singlet *He* I λ 6678, not shown, having the same laboratory intensity as λ 5015, appears in the star with much the same strength and profile as λ 5015. It is possible that a narrow faint absorption line is superposed over the broad line. If this line is real it is probably due to the shell, but the evidence is not complete.

Struve and Wurm report that in φ Persei λ 3965 is always sharp. We should expect, therefore, that λ 5015 should also be sharp in this star. Actually, however, it is absent or present only as a very faint, broad line. The other singlet lines in the visual region (λλ 4922, 5047, and 6678) likewise appear absent or, at most, very faint. The triplet D_3 line, however, is fairly strong. This weakness of the singlets relative to the triplets in φ Persei is confirmed, but the fact that λ 5015 behaves as do the other singlet lines is significant and puzzling. The emission line near λ 5015 in φ Persei is λ 5018 of ionized iron, and it may affect the appearance of λ 5015. The lines λ 4923 and λ 5169 ($a^6S - z^6P$) of *Fe* II are also present in emission. It may be noted in passing that these lines have about the same relative intensities in φ Persei as they had in Nova Herculis,[2] λ 5169 being distinctly the strongest.

In absorption these lines are reported about equal by Marshall[3] in the late B- and early A-type stars but weak or absent in the early B stars. In ζ Tauri λ 5169 is very weak, but there is a distinct emission at λ 5018 which may affect the appearance of λ 5015 by blending. However, the evidence suggests that λ 5015 is not appreciably different in behavior from the other singlet lines of helium in ζ Tauri and φ Persei. The behavior of λ 3965, arising from the same level, becomes thus still more puzzling.

J. A. Hynek

Perkins Observatory
April 1939

THE NEBULOSITY NEAR S MONOCEROTIS

The photograph reproduced in Plate XXVI was obtained on February 15, 1939, with the 24-inch reflector of the Yerkes Observatory. The emulsion used was Eastman Ortho Press. The central

[2] *Contr. Perkins Obs.*, No. 2, p. 24, 1935. [3] *Ap. J.*, **82**, 97, 1935.

portion of the nebula shown in Dr. Van Biesbroeck's photograph, Plate XXVII, is overexposed. An interesting feature of this nebula is the comet-shaped dark marking south of the main nebulosity which shows a conspicuous luminous rim of the type described by Struve.[1]

W. W. MORGAN
FRANCES SHERMAN

YERKES OBSERVATORY

THE NEBULOSITY NEAR S MONOCEROTIS

In the course of the first tests of the 82-inch telescope the nebulosity near S Monocerotis (Pl. XXVII) was photographed at the prime focus on March 13, 1939, with an exposure of five minutes. This bright nebula is particularly interesting because of the conspicuous absence of nebulous matter near two of the stars imbedded in the nebula. This is a well-known phenomenon in several other emission nebulae.

G. VAN BIESBROECK

McDONALD OBSERVATORY

PHOTOGRAPH OF A DIFFUSE NEBULA IN ORION

A small nebula, photographed by H. A. Lower[1] has been examined by Struve and Elvey[2] with the nebular spectrograph of the McDonald Observatory (No. 43 of their list). It has been photographed at the Yerkes Observatory with the 24-inch reflector on Agfa Super-Pan Press film. A Wratten Ciné-Red filter was used to cut out radiation from the night sky to the violet of λ 6000. An exposure of two hours on March 17, 1939, shows the lumpy central part, which, as Struve and Elvey point out, is considerably brighter than the rest (Pl. XXVIII). A faint extension northward is also shown. The star BD+15°1079 lies within the brighter portion; BD+15°1075 lies a little outside.

JOHN A. O'KEEFE

YERKES OBSERVATORY
March 1939

ERRATUM

In the January issue, page 121, in Table 1, No. 28, under "Identification": Ross 26 should read Ross 25.

[1] *Ap. J.*, **85**, 208, 1937.

[1] *Ap. J.*, **89**, Pl. XIV, 1939. [2] *Ap. J.*, **89**, 1939.

PLATE XXVII

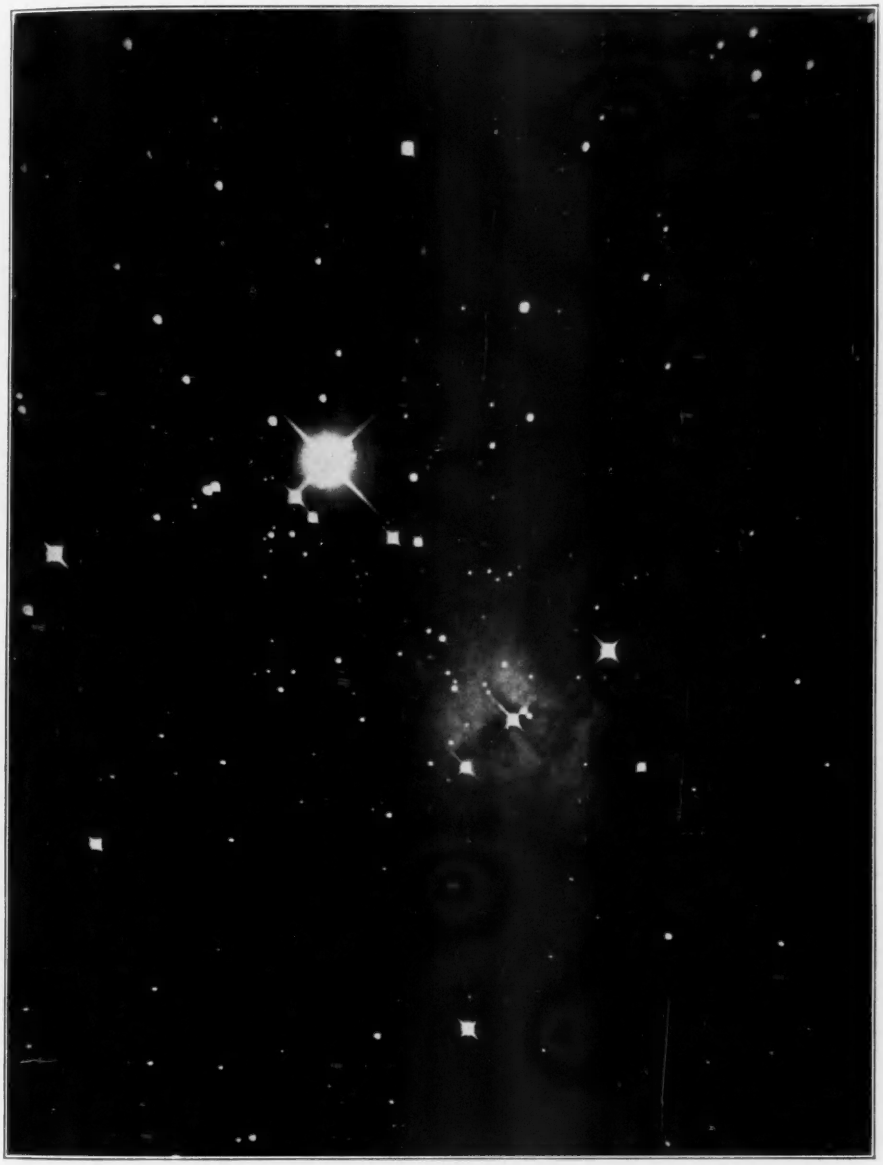

THE BRIGHT NEBULOSITY SOUTH OF S MONOCEROTIS

PLATE XXVIII

LOWER'S DIFFUSE NEBULA IN ORION. SCALE 20″ PER MILLIMETER